Environment International 208 (2026) 110090

Contents lists available at ScienceDirect

Environment International

journal homepage: www.elsevier.com/locate/envint

Full length article

The joint impact of temperature, humidity, and air pollution on COVID-19 incidence: a multi-country time-series study in 439 cities

Keita Wagatsuma [a,b,*], Denise Feurer [c,d], Wenhua Yu [e,f], Rongbin Xu [e,f], Tim Riffe [g,h,i], Maxi Stella Kniffka [i,j], Enrique Acosta [i,k], Ben Armstrong [l], Malcolm Mistry [m,n], Rachel Lowe [o,p,q], Dominic Royé [r,s], Masahiro Hashizume [t,u], Aurelio Tobias [t,v], Ana Maria Vicedo-Cabrera [w,x], Lina Madaniyazi [t], Chris Fook Sheng Ng [u], Carmen Íñiguez [y], Martina S. Ragettli [z,aa], Eric Lavigne [ab,ac], Patricia Matus Correa [ad], Nicolás Valdés Ortega [ad], Jan Kyselý [ae,af], Aleš Urban [ae,af], Hans Orru [ag], Ene Indermitte [ag], Marek Maasikmets [ah], Susanne Breitner-Busch [ai], Alexandra Schneider [ai], Yasushi Honda [aj,ak], Barrak Alahmad [al], Antonella Zanobetti [al], Joel Schwartz [al], Gabriela Carrasco [am], Iulian Horia Holobâca [an], Ho Kim [ao], Whanhee Lee [ap], Michelle L. Bell [aq], Noah Scovronick [ar], Fiorella Acquaotta [as], Micheline de Sousa Zanotti Stagliorio Coelho [at], Magali Hurtado Diaz [au], Eunice Elizabeth Félix Arellano [au], Paola Michelozzi [av], Massimo Stafoggia [av], Francesca de'Donato [av], Shilpa Rao [aw], Xerxes Seposo [ax], Shilu Tong [ay,az], Jochem Klompmaker [aaa], Yuming Guo [e,f], Pierre Masselot [m], Antonio Gasparrini [m], Francesco Sera [aab]

[a] Division of International Health (Public Health), Graduate School of Medical and Dental Sciences, Niigata University, Niigata, Japan
[b] Institute for Research Administration, Niigata University, Niigata, Japan
[c] Unit of Biostatistics, Epidemiology and Public Health (UBEP), University of Padua, Padua, Italy
[d] Interdepartmental Research Center of Geomatics (CIRGEO), University of Padua, Padua, Italy
[e] Department of Epidemiology and Preventive Medicine, School of Public Health and Preventive Medicine, Monash University, Melbourne, Australia
[f] Climate, Air Quality Research Unit, School of Public Health and Preventive Medicine, Monash University, Melbourne, Australia
[g] Universidad del País Vasco (UPV/EHU), Leioa, Spain
[h] Ikerbasque (Basque Foundation for Science), Bilbao, Spain
[i] Max Planck Institute for Demographic Research, Rostock, Germany
[j] Universität Rostock, Germany
[k] Centre d'Estudis Demogràfics, Bellaterra, Spain
[l] Department of Public Health, Environments and Society, London School of Hygiene & Tropical Medicine, London, UK
[m] Environment & Health Modelling (EHM) Lab, Department of Public Health, Environments and Society, London School of Hygiene & Tropical Medicine, London, UK
[n] Department of Economics, Ca' Foscari University of Venice, Venice, Italy
[o] Barcelona Supercomputing Center (BSC), Barcelona, Spain
[p] Catalan Institution for Research and Advanced Studies (ICREA), Barcelona, Spain
[q] Centre on Climate Change & Planetary Health and Centre for Mathematical Modelling of Infectious Diseases, London School of Hygiene & Tropical Medicine, London, UK
[r] CIBERESP, Madrid, Spain
[s] Biological Mision of Galicia (MBG), Spanish Council for Scientific Research (CSIC), Madrid, Spain
[t] School of Tropical Medicine and Global Health, Nagasaki University, Japan
[u] Department of Global Health Policy, Graduate School of Medicine, The University of Tokyo, Tokyo, Japan
[v] Institute of Environmental Assessment and Water Research (IDAEA), Spanish Council for Scientific Research (CSIC), Barcelona, Spain
[w] Institute of Social and Preventive Medicine, University of Bern, Bern, Switzerland
[x] Oeschger Center for Climate Change Research, University of Bern, Bern, Switzerland
[y] Department of Statistics and Computational Research, Universitat de València, València, Spain
[z] Swiss Tropical and Public Health Institute, Allschwil, Switzerland
[aa] University of Basel, Basel, Switzerland

* Corresponding author at: Division of International Health (Public Health), Graduate School of Medical and Dental Sciences, Niigata University, 1-757 Asahimachi-dori, Chuo-ku, Niigata City, Niigata 951-8510, Japan.
E-mail address: waga@med.niigata-u.ac.jp (K. Wagatsuma).

https://doi.org/10.1016/j.envint.2026.110090
Received 14 October 2025; Received in revised form 6 January 2026; Accepted 19 January 2026
Available online 24 January 2026

[ab] School of Epidemiology and Public Health, Faculty of Medicine, University of Ottawa, Ottawa, Canada
[ac] Environmental Health Science and Research Bureau, Health Canada, Ottawa, Canada
[ad] Department of Public Health, Universidad de los Andes, Santiago, Chile
[ae] Institute of Atmospheric Physics of the Czech Academy of Sciences, Prague, Czech Republic
[af] Faculty of Environmental Sciences, Czech University of Life Sciences, Prague, Czech Republic
[ag] Institute of Family Medicine and Public Health, University of Tartu, Tartu, Estonia
[ah] Estonian Environmental Research Centre, Tallinn, Estonia
[ai] Institute of Epidemiology, Helmholtz Zentrum München–German Research Center for Environmental Health (GmbH), Neuherberg, Germany
[aj] Center for Climate Change Adaptation, National Institute for Environmental Studies, Tsukuba, Japan
[ak] Faculty of Health and Sport Sciences, University of Tsukuba, Tsukuba, Japan
[al] Department of Environmental Health, Harvard T.H. Chan School of Public Health, Harvard University, Boston, USA
[am] Institute of Tropical Medicine "Alexander von Humboldt", Universidad Peruana Cayetano Heredia, Lima, Peru
[an] Faculty of Geography, Babes-Bolyai University, Cluj-Napoca, Romania
[ao] Department of Public Health Science, Graduate School of Public Health, & Institute of Health and Environment, Seoul National University, Seoul, South Korea
[ap] School of Biomedical Convergence Engineering, Pusan National University, South Korea
[aq] School of the Environment, Yale University, New Haven, CT, USA
[ar] Department of Environmental Health. Rollins School of Public Health, Emory University, Atlanta, USA
[as] Department of Earth Sciences, University of Torino, Italy
[at] Laboratory of Environmental and Experimental Pathology, University of São Paulo, Faculty of Medicine, Brazil
[au] Department of Environmental Health, National Institute of Public Health, Cuernavaca, Morelos, Mexico
[av] Department of Epidemiology, Lazio Regional Health Service, Rome, Italy
[aw] Norwegian Institute of Public Health, Oslo, Norway
[ax] Department of Hygiene, Graduate School of Medicine, Hokkaido University, Sapporo, Japan
[ay] National Institute of Environmental Health, China CDC, Beijing, China
[az] School of Public Health and Social Work, Queensland University of Technology, Brisbane, Australia
[aaa] National Institute for Public Health and the Environment (RIVM), Bilthoven, Netherlands
[aab] Department of Statistics, Computer Science and Applications "G. Parenti", University of Florence, Florence, Italy

ARTICLE INFO

Keywords:
Humidex
$PM_{2.5}$
COVID-19
MCC Collaborative Research Network
Two-stage design
Effect modification

ABSTRACT

Several studies have explored the short-term effects of environmental stressors on coronavirus disease 2019 (COVID-19) transmission and severity. However, evidence on the interactive effects of meteorological conditions and air pollution remains limited and geographically variable. We therefore aimed to quantify the independent and interactive effects of short-term exposure to humidex, a composite index of temperature and relative humidity, and fine particulate matter $\leq$ 2.5 μm ($PM_{2.5}$) on daily COVID-19 incidence across multiple cities and in multiple countries. Daily time-series data on confirmed COVID-19 cases, meteorological factors, and $PM_{2.5}$ concentrations were collected from 439 cities in 22 countries during January 2020–August 2022 as part of the Multi-Country Multi-City Collaborative Research Network. A two-stage design was applied: first, city-specific quasi-Poisson models with distributed lag non-linear models estimated exposure–response associations; second, multilevel random-effects *meta*-analyses pooled city-specific estimates. Effect modification by $PM_{2.5}$ was assessed using a product term between non-linear humidex function and linear $PM_{2.5}$ function. Approximately 95.1 million confirmed COVID-19 cases were analyzed. Lower humidex values (0.1 °C versus 15.1 °C) were associated with increased daily cases (relative risk [RR]: 1.1192, 95% confidence interval [CI]: 1.0214–1.2262). A 10 $\mu g/m^3$ increase in $PM_{2.5}$ over the current and preceding 2 days was associated with a modest increase in daily cases (RR: 1.0079, 95% CI: 1.0001–1.0161). No statistically significant interaction between humidex and $PM_{2.5}$ was observed. Short-term exposure to cold–dry conditions and elevated $PM_{2.5}$ independently increased COVID-19 incidence, highlighting the need to consider both thermal environment and air quality when designing climate-resilient public health responses. These findings enhance understanding of how climate-related environmental stressors influence COVID-19 transmission.

1. 1 Introduction

Since the initial report of a cluster outbreak of severe acute respiratory syndrome coronavirus 2 (SARS-CoV-2) in Wuhan, China in December 2019, coronavirus disease 2019 (COVID-19) has remained a major public health concern(Heymann and Shindo, 2020; Oshitani, 2022). Despite more than 5 years passing and the disease transitioning toward endemicity, it continues to cause substantial morbidity, mortality, and economic burdens worldwide (Chakraborty et al., 2025; Spinner et al., 2025). In response to the emergence and rapid spread of novel variants with varying transmissibility, such as delta and Omicron, a wide range of non-pharmaceutical interventions (NPIs) and mass vaccination programs have been implemented globally (Ge et al., 2022). By the end of 2024, World Health Organization reported more than 770 million confirmed COVID-19 cases and over 7 million deaths across 234 countries (World Health Organization, 2025). These figures highlight the urgent need to understand the factors driving SARS-CoV-2 transmission to mitigate its impact and reduce the strain on governments and healthcare systems. At the same time, the pandemic and related containment measures have themselves altered environmental conditions, with widespread lockdowns temporarily reducing ambient air pollution, reshaping economic activities, and raising concerns about the broader environmental and societal consequences of COVID-19 (Gautam, 2020; Gautam and Hens, 2020; Bherwani et al., 2020, 2021).

The relationship between ambient meteorological factors and COVID-19 transmission dynamics remains a key focus of research and debate (Ford et al., 2022). Numerous studies have consistently indicated that temperature and humidity (both relative and absolute) are critical determinants that influence not only the survival and transmission of SARS-CoV-2 but also individual susceptibility, immune responses, and human behavior (Chong et al., 2024; Feurer et al., 2024; Ma et al., 2021; Nottmeyer et al., 2023; Sera et al., 2021; Wang et al., 2023; Xu et al., 2021). An early systematic review, published in 2020, which evaluated 61 studies on the association between COVID-19 and meteorological conditions and reported that low temperature and low humidity were linked to an increased risk of COVID-19 (Briz-Redón and Serrano-Aroca, 2020). These findings have been further corroborated by a recent global time-series analysis examining the association between meteorological

factors and COVID-19 incidence across 439 cities in 22 countries through the summer of 2022 (Feurer et al., 2024). Most epidemiological studies examining thermal stress and COVID-19 transmission have relied on temperature as the primary exposure metric. However, composite thermal indices that combine multiple meteorological factors may more accurately characterize the operative thermal environment (McGregor, 2012a). A variety of such indices have been developed to synthesize environmental determinants of thermal stress including temperature, humidity, wind speed, atmospheric pressure, and solar radiation into a single measure. For example, the heat index which combines air temperature and relative humidity to represent perceived temperature, is straightforward to compute and aligns well with thermal under moderate conditions. However, its validity deteriorates under conditions of extreme cold or very low humidity (McGregor, 2012b; Urban et al., 2021; Xu et al., 2025). Therefore, more advanced thermal indices based on the human heat balance equation have been developed (Urban et al., 2021). The wet-bulb globe temperature (WBGT) integrates multiple meteorological variables to provide a comprehensive measure of heat stress. However, its calculation is relatively complex and accounts only minimally for inter-individual variability (Cheuvront et al., 2015; Urban et al., 2021; Xu et al., 2025). Composite indices that capture both heat and cold stresses such as the universal thermal climate index (UTCI) incorporate a broad range of environmental factors and offer a dynamic representation of real-world thermal conditions, though their computation typically requires detailed input data (McGregor, 2012a). In recent decades, to better understand the combined effects of temperature and humidity on infectious diseases such as influenza, hand, foot, and mouth disease (HFMD), tuberculosis, and bacillary dysentery, several studies have increasingly employed humidex, a composite index that integrates both variables (Fan et al., 2020; Gao et al., 2025; Li et al., 2024; Zhao et al., 2021). In general, the thermal perception at a given temperature varies markedly with humidity, and an index that jointly incorporates temperature and humidity can better capture human discomfort than either variable in isolation. Compared with other complex composite indices, humidex does not require sophisticated measuring tools and is easier to calculate. This makes it broadly applicable for assessing of real-world thermal conditions in both cold and hot environments. However, evidence on the short-term effect of humidex on COVID-19 incidence remains limited with few studies addressing this relationship.

Although systematic evidence is limited, short-term exposure to ambient air pollutants may influence COVID-19 morbidity and mortality rates. Similar patterns have been reported for other infectious diseases including influenza, HFMD, and tuberculosis, where short-term fluctuations in air pollution were linked to changes in incidence (Li et al., 2019; Rittweger et al., 2022; Zhan et al., 2023; R. Zhang et al., 2023). A time-series study conducted in early 2020 across 120 Chinese cities found that air pollutants, fine particulate matter ≤ 2.5 μm ($PM_{2.5}$), fine particulate matter ≤ 10 μm (PM_{10}), carbon monoxide (CO), nitrogen dioxide (NO_2), and ozone (O_3), were associated with an increased risk of COVID-19 infection (Zhu et al., 2020). In the United States, ecological studies reported that counties with higher long-term $PM_{2.5}$ exposure had elevated COVID–19 mortality rates (X. Wu et al., 2020), a finding supported by a large-scale population-based study of more than four million cases in Italy (Stafoggia et al., 2023). An individual-level case-crossover study in the United States further demonstrated that short-term exposure to $PM_{2.5}$ increased the risk of COVID-19 mortality (Kim et al., 2022). Recent systematic reviews and *meta*-analyses have consistently confirmed significant associations between short-term exposure to $PM_{2.5}$, PM_{10}, and NO_2 and higher COVID–19 mortality (Yu et al., 2024). Additionally, ecological analyses from Asian settings suggest that elevated air pollution may aggravate COVID-19 lethality, further supporting a potential association between particulate matter exposure and adverse clinical outcomes (Gupta et al., 2021). Moreover, air pollution may modulate the health effects of meteorological factors not only through direct physiological impacts, but also by increasing population vulnerability (Rai et al., 2023). However, evidence specifically examining the modifying effects of air pollutants on the relationship between meteorological factors and COVID–19 incidence remain limited.

Although numerous epidemiological studies have examined associations between meteorological factors, air pollution, and COVID-19 incidence, most have focused on their independent effects, with relatively few exploring potential interactions or considering composite thermal indices. Additionally, many studies have not accounted for non-linear or lagged relationships between exposure and health outcomes, lacked adjustment for time-varying or location-specific confounders, and were limited by short observation periods or geographically restricted data sets factors that constrain the generalizability of their findings. Consequently, significant evidence gaps remain regarding the interactive effects of meteorological factors and $PM_{2.5}$ on COVID-19 incidence across diverse climatic and socioeconomic contexts. To address these gaps, we conducted a multi-location time-series study using an extensive dataset from 439 cities across 22 countries, compiled by the Multi-Country Multi-City (MCC) Collaborative Research Network, an international consortium generating global evidence environmental stressors, climate, and health (Gasparrini et al., 2024). This study applied city-level time-series models to systematically investigate both the independent and interactive effects of humidex and $PM_{2.5}$ on COVID-19 incidence worldwide. Humidex itself is a long-established composite index of temperature and relative humidity; here we extend its use to a large multi-country analysis of COVID-19 jointly with air pollution. To the best of our knowledge, this is the first global analysis to quantify these short-term effects and their potential interaction across diverse settings worldwide. Our findings provide additional insights into the health impacts of co-exposure to humidex and air pollution, which can inform the environmental component of early warning and surveillance frameworks for COVID-19 and other respiratory infections, even as the pandemic evolves toward endemicity.

2. Materials and methods

2.1. Study design and data collection

Daily time-series data on confirmed COVID-19 cases, meteorological factors, and $PM_{2.5}$ concentrations were obtained for 439 cities across 22 countries. For each city, we used the daily number of confirmed COVID-19 cases as reported in the corresponding national or regional surveillance system, typically based on the date of report or notification, rather than the date of infection. These data were sourced from publicly accessible repositories and supplemented with datasets provided by the MCC Collaborative Research Network (Gasparrini et al., 2024). The MCC database has been widely used to evaluate associations between meteorological factors and COVID-19 incidence (Feurer et al., 2024; Nottmeyer et al., 2023; Sera et al., 2021). Specifically, daily case data were initially compiled for 458 cities across 22 countries between January 1, 2020, and August 31, 2022, as previously described (Feurer et al., 2024). For this study, we restricted the analysis to MCC cities with complete indicator datasets and excluded those with $> 5\%$ missing data or unexplained anomalies after visual inspection. The final dataset comprised 439 cities in 22 countries. Details of the cities and data sources are provided in Table S1.

We obtained hourly ambient meteorological data, including air temperature (°C), relative humidity (%), total precipitation (mm), and ultraviolet radiation (J/m^2), from the ERA5-Land reanalysis dataset, developed by the European Center for Medium-Range Weather Forecasts and accessible via the Copernicus Climate Data Store (https://cds.climate.copernicus.eu/datasets/reanalysis-era5-single-levels?tab=overview)(Feurer et al., 2024; Nottmeyer et al., 2023). This dataset provides global coverage at a spatial resolution of $0.1° \times 0.1°$ (approximately 11 km × 11 km at the equator). For each of the 439 cities included in the analysis, daily averages of the mean temperature, dew point temperature (measured 2 m above ground level), total

precipitation, and ultraviolet radiation were derived from the grid cell corresponding to the city's geographical centroid. Relative humidity was then calculated from air temperature and dew point temperature using the "humidity" R package.

To represent the combined effects of temperature and atmospheric moisture perceived by humans, we calculated the daily humidity, an index developed by Canadian meteorologists that integrates temperature and relative humidity into a single value (d'Ambrosio Alfano et al., 2011; Gao et al., 2025). The daily time-series of humidex (°C) was computed using the following formula:

$$Humidex = T + \frac{5}{9} \times \left\{ 6.11 \times 10^{\left(\frac{7.5 \times T}{237+T}\right)} \times \frac{RH}{100} - 10 \right\} \quad (1)$$

where T denotes the daily mean temperature and RH represents the daily relative humidity.

Daily surface-level $PM_{2.5}$ concentrations (μg/m^3) for all 439 cities were extracted from a global dataset developed using a deep ensemble machine learning framework, as previously described (W. Yu et al., 2024b; Yu et al., 2023, 2022). The dataset provides daily estimates at a spatial resolution of 0.1° × 0.1° (approximately 11 × 11 km at the equator) derived from ground-based observations collected at 5,446 monitoring sites across 65 countries between 2000 and 2019. The model demonstrated strong predictive performance, with daily $PM_{2.5}$ estimates showing high agreement with ground measurements (cross-validation $R^2 = 0.91$; root-mean-square error of 7.86 μg/m^3) in independent validation data.

We also accounted for potential confounders that could influence the association between environmental exposure and COVID-19 incidence (Feurer et al., 2024; Nottmeyer et al., 2023). To capture temporal variation in public health and social measures (PHSMs), we obtained the Government Stringency Index (GSI) from the Oxford COVID-19 Government Response Tracker (OxCGRT) at the country level (https://www.bsg.ox.ac.uk/research/covid-19-government-response-tracker) (Feurer et al., 2024; Nottmeyer et al., 2023). The GSI is a composite indicator ranging from 0 (no restrictions) to 100 (maximum stringency), incorporating daily updates on government policies, such as school and workplace closures, mobility restrictions, economic support, and testing strategies. To account for changes in population immunity over time, we extracted daily country-level vaccination data from the World Database (https://ourworldindata.org) (Feurer et al., 2024). The vaccination variable was defined as the proportion of individuals fully vaccinated, i.e., those who had completed the primary vaccination regimen (typically one or two doses, depending on the vaccine type). These values were expressed as the ratio of fully vaccinated individuals to the total national population. As all data used in this study were aggregated, anonymized, and derived from publicly accessible sources and the MCC Collaborative Research Network, ethical approval was not required.

2.2. Statistical analysis

2.2.1. Descriptive analysis

Descriptive statistics were compiled at both country and city levels. At the country level, we summarized the number of cities included, cumulative confirmed COVID-19 cases, and the daily mean and range of environmental exposures, including humidex, $PM_{2.5}$ concentrations, total precipitation, ultraviolet solar radiation, OxCGRT GSI, and vaccination coverage. The same variables were summarized at the city level to capture within-country variation.

2.2.2. Two-stage time-series design

We adopted an extended two-stage design, commonly applied in previous multi-center time-series studies (Sera and Gasparrini, 2022). In the first stage, we used city-specific time-series regression models with the daily number of newly confirmed COVID-19 cases in each city as the outcome and humidex and $PM_{2.5}$ concentrations as the main exposures, while accounting for time-varying confounders. In the second stage, multivariate *meta*-regression was used to pool the city-specific estimates and derive the overall exposure–lag–response association curve. Modelling choices were pre-followed based on previous MCC studies using an overlapping dataset and applied identically to all cities to enhance reproducibility (Feurer et al., 2024; Nottmeyer et al., 2023; Sera et al., 2021).

In the first stage, we fitted city-specific main models including both environmental stressors, i.e., humidex and $PM_{2.5}$. Specifically, we used a generalized linear model with a quasi-Poisson distribution and a logarithmic link to account for overdispersion, incorporating a distributed lag non-linear model (DLNM) to simultaneously capture non-linear exposure–response relationships and the lagged effects (Gasparrini, 2011). For humidex, the exposure–response relationship was modeled using a second-degree polynomial function, while the lag–response relationship was specified with a natural cubic spline with two internal knots placed at equally spaced values on a logarithmic scale, consistent with previous work (Nottmeyer et al., 2023). A maximum lag of 14 days was applied in the main analysis, based on short-term health effects of meteorological factors on COVID-19 incidence (Feurer et al., 2024; Nottmeyer et al., 2023). Recognizing that temperature is the most used thermal exposure metric, we reconstructed the main model by replacing humidex with temperature and compared model fit using the sum of the quasi-Akaike information criterion (qAIC) across all cities (Armstrong et al., 2019). The humidex specification yielded a lower total qAIC than that of the temperature-based model (8,390,639 versus 8,397,653), supporting its use as the preferred exposure metric. For $PM_{2.5}$, the exposure–response relationship was modeled as linear and the lag–response relationship was assessed using an unconstrained (integer) model with separate coefficients (O'Brien et al., 2023). Preliminary analyses modeled $PM_{2.5}$ lags of up to 14 days using a natural cubic spline with two internal knots placed at equally spaced values on the logarithmic scale; however, associations were mainly confined to the first few days (Fig. S1). Therefore, a maximum lag of 2 days (0, 1, and 2 days) was applied in the main analysis, consistent with previous studies on the short-term health effects of ambient air pollution (Liu et al., 2019; Masselot et al., 2024; O'Brien et al., 2023). The same functional forms and lag structure for humidex and $PM_{2.5}$ were applied in all cities.

Several potential confounders were accounted for in the main model (Feurer et al., 2024; Nottmeyer et al., 2023). To adjust for variations in case reporting and behavioral or operational factors across the week, such as social activity patterns or testing capacity, indicator variables for each day of the week were included. Additionally, three time-varying covariates were incorporated. First, intra- and inter-annual trends in COVID-19 incidence were modeled using a natural spline function of time with 10 degrees of freedom (df) per year. Second, to account for potential confounders related to PHSMs and population immunity, distributed lag linear models for OxCGRT GSI and vaccination coverage were included, allowing for lag effects of up to 14 days. Third, to capture underlying transmission dynamics, given an estimated incubation period of approximately 6 days, autoregressive terms were introduced by including the natural logarithm of COVID-19 cases plus one, lagged by 1–6 days (Imai et al., 2015; McAloon et al., 2020; Wu et al., 2022). The same set of confounders was specified for all city-specific models.

In the second stage, we applied a multilevel random-effects *meta*-analytic model to pool city-specific estimates of humidex and $PM_{2.5}$ using restricted maximum likelihood estimation (Sera et al., 2019; Sera and Gasparrini, 2022). Random effects were specified for groups defined by the intersection of the country and Köppen–Geiger climate zone (Peel et al., 2007). Residual heterogeneity across cities was assessed using a multivariate extension of Cochran's Q-test and quantified with the I^2 statistic. From this *meta*-analysis model, we generated pooled overall exposure–response curves for COVID-19 incidence, expressed as relative risks (RRs) at the 10th and 90th percentiles of exposure, using the median humidex and 0 μg/m^3 for $PM_{2.5}$ as reference, with corresponding 95%

confidence intervals (CIs) to quantify uncertainty. Effect estimates are reported as RRs with 95% CIs; humidex effects pertain to daily COVID-19 cases, whereas $PM_{2.5}$ effects are expressed as the RR per 10 μg/m^3 increase in concentration. In addition to estimating exposure–response associations, we quantified the attributable burden of COVID-19 cases due to short-term exposure to $PM_{2.5}$, expressed as the attributable number (AN) and attributable fraction (AF) (O'Brien et al., 2023). The total AN was obtained by summing the daily contributions over the entire study period, and the AF was calculated as the ratio of this total AN to the total number of observed cases. Empirical confidence intervals (eCIs) for the AN were derived via Monte–Carlo simulations ($n = 1{,}000$), assuming a multivariate normal distribution for the estimated coefficients of the exposure–response functions in the regression model, and eCIs for the AF were obtained by dividing the simulated AN values by the total number of cases.

2.3. Interaction analysis

To assess whether the humidex–COVID-19 association varied with $PM_{2.5}$ concentration, we extended the main model to include a product term between the cross-basis function of humidex and a linear term for the 0–2-day moving average of $PM_{2.5}$, along with the main terms for humidex and $PM_{2.5}$ (Min et al., 2025). The exposure–response curves of humidex were predicted at the 10th (low concentration) and 90th (high concentration) percentiles of the overall $PM_{2.5}$ distribution across all cities. To quantify the degree of effect modification, we calculated the ratio of relative risks (RRRs) with corresponding 95% CIs.

2.4. Sensitivity analysis

We conducted a series of sensitivity analyses to evaluate the robustness of our main findings under different modeling choices and assumptions. First, we varied the maximum lag period from 14–21 days for humidex, and from 2–7 days for $PM_{2.5}$ exposure. Second, we tested the sensitivity to temporal trend control by changing the df for the natural cubic spline of calendar time from 10 to 7 df per year. Third, we adjusted for potential confounders, including daily mean ultraviolet radiation, and precipitation using natural cubic splines with three df in the first-stage model. Fourth, we explored different functional forms for the exposure–response associations, specifying a linear term for humidex and a second-degree polynomial function for $PM_{2.5}$. Fifth, to assess independent effects, we fitted single-exposure models, for humidex or $PM_{2.5}$, and evaluated their associations with COVID-19 incidence. Sixth, to support the use of humidex, we examined the exposure–response curve for temperature on COVID-19 incidence. Seventh, to assess the influence of lag structure on the estimated effect modification, we re-fitted the $PM_{2.5}$ models using alternative lag windows, replacing the 0–2-day moving average with 0–1 and 0–3-day averages. Finally, to test the sensitivity of exposure categorization, we defined low and high $PM_{2.5}$ concentrations as the 1st and 99th percentiles of the distribution. Additionally, to address potential differences across SARS-CoV-2 variants, we conducted a sensitivity analysis stratified by dominant strain period. Following previous study (Feurer et al., 2024), we considered three main variants, Initial, Delta, and Omicron, and, for each country and calendar month, assigned the dominant strain as the variant accounting for the largest share of sequenced cases. In this context, "Initial" refers to the early pandemic period, when genomic surveillance was limited and several mutant lineages co-circulated before any specific variant became the dominant driver of transmission. We then re-estimated the pooled overall exposure–response curves for humidex and $PM_{2.5}$ separately within each dominant strain period to assess the consistency of the associations across variants. In an additional analysis, we reparametrized the interaction model by treating $PM_{2.5}$ as the main exposure and humidex as the effect modifier and estimated the cumulative RR per 10 μg/m^3 increase in $PM_{2.5}$ at the 10th and 90th percentiles of humidex, together with the corresponding RRR curve. Statistical significance of the p-value was < 0.05, based on a two-tailed test. All analyses were conducted in R statistical software, version 4.2.0 (The R Foundation for Statistical Computing, Vienna, Austria), using "dlnm" and "mixmeta" R packages. The code for the complete analysis is available from the corresponding author on reasonable request.

3. Results

3.1. Descriptive analysis

This analysis included approximately 95.1 million confirmed COVID-19 cases reported across 439 cities in 22 countries spanning five continents as of August 31, 2022. The geographical distribution of these cities and the aggregated national time-series of daily case counts are shown in Figs. 1 and 2. Most countries experienced multiple epidemic waves associated with successive SARS-CoV-2 variants, with a prominent peak observed during the emergence of the Omicron variant in late 2021 and early 2022. A complete list of study locations is provided in Table S2. Table 1 summarizes COVID-19 cases counts, environmental exposure, government stringency index values, and vaccination coverage during the study period. The cumulative number of cases ranged from 163,026 in Australia to 32,572,370 in the United States. Substantial heterogeneity in environmental exposures was observed both across and within countries. The daily mean humidex ranged from 5.1 °C in Canada to 38.1 °C in Singapore. The highest average $PM_{2.5}$ concentrations were recorded in Singapore (42.1 μg/m^3) and Chile (41.1 μg/m^3), while Australia and Estonia reported the lowest levels (<7 μg/m^3). Ultraviolet radiation was greatest in tropical settings such as Mexico, Peru, and Kuwait, whereas precipitation was highest in Singapore and the Philippines and lowest in Kuwait. Temporal trends of the environmental variables by country are presented in Fig. S2–S5. As expected, tropical and subtropical countries (e.g., Brazil, Chile, Mexico, Peru, the Philippines, Singapore, and South Africa) exhibited limited seasonal variability in humidex, while $PM_{2.5}$ concentrations showed no distinct temporal pattern. Correlation analysis revealed a weak negative association between humidex and COVID-19 cases (Spearman's $\rho = -0.10$), and a weak positive correlation with $PM_{2.5}$ concentrations (Spearman's $\rho = 0.10$; Fig. S6). Government response patterns are shown in Fig. S7. Most countries implemented strict mitigation measures in early 2020, which were gradually relaxed by mid-year, although several reinstated stringent controls later that year. The highest mean stringency levels were recorded in Peru (69.2%), the Philippines (67.3%), and Chile (62.0%), whereas Estonia (37.9%), and Norway (41.6%) adopted relatively lenient policies. Trends in vaccination coverage are shown in Fig. S8. Chile and Singapore achieved the highest mean daily coverages (42.3% and 40.0%, respectively), while South Africa (10.7%) and Romania (17.3%) had the lowest.

3.2. Short-term associations of COVID-19 cases with humidex and $PM_{2.5}$ concentration

Fig. 3 presents the pooled association curves derived from the *meta*-analytical models assessing humidex and $PM_{2.5}$ concentrations. Overall, lower humidex levels were associated with an increased risk of COVID-19. Specifically, exposure at the 10th percentile (0.1 °C) correspond to a 1.1192-fold (95% CI: 1.0214–1.2262) higher risk compared with the median reference value of 15.1 °C (Fig. 3A). In contrast, exposure at the 90th percentile (33.3 °C), was associated with a reduced risk (RR: 0.8311, 95% CI: 0.7428–0.9510). The corresponding cumulative lag–response curve indicated elevated RRs at lags of 2–14 days for the 10th percentile (Fig. 3C) and a declining risk trend at lags of 3–14 days for the 90th percentile (Fig. 3E). Substantial heterogeneity was observed in the *meta*-analysis (Cochran's Q-test, p-value < 0.001; $I^2 = 75.5\%$). For $PM_{2.5}$, a positive association with COVID-19 incidence was observed. A 10 μg/m^3 increase in $PM_{2.5}$ concentration over the current and two

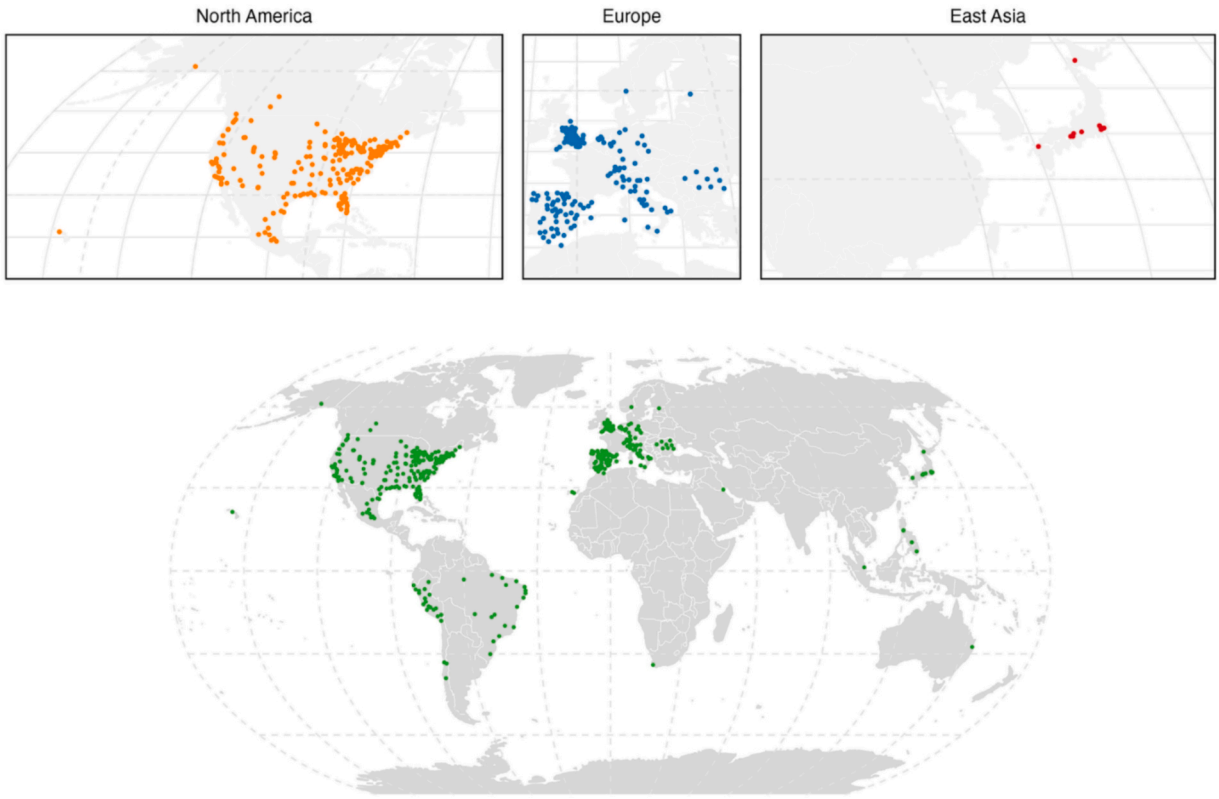

Fig. 1. World map showing the included cities color-coded by region.

preceding days was associated with an RR of 1.0079 (95% CI: 1.0001–1.0161; Fig. 3B). In terms of attributable burden, we estimated that approximately 1.81% (95% eCI: 0.75–2.42) of all confirmed COVID-19 cases were attributable to $PM_{2.5}$ exposure, corresponding to 1,675,070 additional cases (95% eCI: 699,086–2,230,909) globally. Lag-specific analyses for both the 10^{th} and 90^{th} percentiles revealed positive associations, with the strongest effect at a 2-day lag (RR: 1.0026 [95% CI: 1.0004–1.0049] and RR: 1.0127 [95% CI: 1.0020–1.0236], respectively), followed by lags 0 and 1 (Fig. 3D and 3F). Heterogeneity was noted in the *meta*-analysis (Cochran's *Q*-test, *p*-value < 0.001; $I^2 = 64.6\%$).

3.3. Modifying effects of $PM_{2.5}$ concentration on the association between humidex and COVID-19 cases

Fig. 4A illustrates the overall cumulative association between humidex and COVID-19 incidence under low and high $PM_{2.5}$ concentrations. Overall, there was minimal evidence of effect modification by $PM_{2.5}$, suggesting that the additional contribution of particulate matter was marginal. At the 10^{th} percentile of humidex (0.1 °C), compared with the median (15.1 °C), the estimated RR was 1.1127 (95% CI: 1.0003–1.2378) under low $PM_{2.5}$ and 1.1139 (95% CI: 1.0185–1.2181) under high $PM_{2.5}$ concentrations. At the 90^{th} percentile (33.3 °C), the corresponding RRs were 0.8328 (95% CI: 0.7146–0.9704) and 0.8446 (95% CI: 0.7291–0.9568), respectively. The effect modification $PM_{2.5}$ concentration is further depicted in Fig. 4B, where the curves represent the RRRs comparing the 10^{th} to the 90^{th} percentile of $PM_{2.5}$ across the humidex range. No evident $PM_{2.5}$ modification was observed across the exposure range based on central estimates.

3.4. Sensitivity analysis

Sensitivity analyses showed that the overall shape of the exposure–response association curve remained broadly consistent across a range of modeling assumptions, with only minor variations in the effect estimates and CIs. These analyses included changes to the maximum lag period (Fig. S9), df for calendar-time adjustment (Fig. S10), the inclusion of additional potential confounders such as ultraviolet radiation and precipitation (Fig. S11), application of alternative functional form for exposure–response modelling (Fig. S12), assessment of humidex and $PM_{2.5}$ using separate univariate models (Fig. S13), comparison of the exposure–response relationship between temperature and COVID-19 incidence (Fig. S14), alternative specifications of the $PM_{2.5}$ exposure window (Fig. S15) and different definitions of low and high $PM_{2.5}$ concentrations (Fig. S16). In sensitivity analyses stratified by the dominant SARS-CoV-2 variant period (Initial, Delta, and Omicron), the cumulative exposure–response curves for humidex and $PM_{2.5}$ were broadly similar across periods, with wide and largely overlapping 95% CIs (Fig. S17). The cumulative RRs per 10 $\mu g/m^3$ increase in $PM_{2.5}$ were similar at low and high humidex levels, and the RRR curve remained close to unity across the $PM_{2.5}$ range (Fig. S18). Overall, these findings support the robustness and reliability of the proposed model across varied parameter specifications.

4. Discussion

To the best of our knowledge, this study represents the most comprehensive epidemiological assessment of the independent and interactive effects of short-term exposure to humidex and $PM_{2.5}$ on COVID-19 incidence, using an extensive dataset of nearly 95 million confirmed cases from 439 cities in 22 countries on five continents. Our global analyses indicate two key findings. First, lower humidex values and higher $PM_{2.5}$ concentrations were associated with an increased risk of COVID-19. Second, we found no compelling evidence that $PM_{2.5}$ levels significantly modified the humidex–COVID-19 association. These findings offer valuable insights for public health strategies aimed at mitigating the impacts of meteorological factors and air pollution on COVID-19 transmission. While humidex has long been used as a

Fig. 2. Time–series of COVID-19 cases aggregated by country over the period.

composite index of temperature and relative humidity, its short-term associations with COVID-19 incidence and its joint effects with $PM_{2.5}$ have, to the best of our knowledge, not previously been examined in a multi-country analysis at this spatial and temporal scale.

Global pooled estimates indicate that lower humidex levels are associated with an increased risk of COVID-19. Specifically, we found evidence of independent associations between temperature, humidity, and COVID-19 incidence on a global scale. This finding is consistent with previous studies that examined the short-term effects of temperature and humidity individually. Employing a range of statistical approaches and country- or region-level datasets, several studies have reported an inverse association between temperature, humidity, and COVID-19 case rates (Sarkodie and Owusu, 2020; Y. Wu et al., 2020; Yuan et al., 2021; Zhang et al., 2021). These findings have been further supported by multi-center analyses conducted in individual countries, including the United States, the United Kingdom, Italy, and Spain, which reported trends broadly consistent with those observed in the present study (Donzelli et al., 2022; Ma et al., 2021; Nottmeyer and Sera, 2021; Rubin et al., 2020). Likewise, two earlier multi-country analyses based on a shorter COVID-19 time-series showed exposure–response curves consistent with our result, despite some differences in geographical coverage and analytical methods (Feurer et al., 2024; Nottmeyer et al., 2023). Additionally, a global study encompassing 2,143 city- and district-level locations across six low- and middle-income countries reported that temperature and humidity exerted both independent and interactive effects on COVID-19 transmission, although the magnitude and direction of these associations varied across climate zones (Wang et al., 2023). Given the ongoing evolution of SARS-CoV-2 to evade prior immunity and its multiple modes of transmission, several biological and behavioral mechanisms may underlie the observed associations with humidex. From a pathogenic perspective, low humidity conditions, characterized by reduced temperature and humidity, may enhance the environmental stability and persistence of SARS-CoV-2 by altering the physical properties of its lipid envelope, thereby prolonging viral viability, and increasing host susceptibility (Chan et al., 2011; Polozov et al., 2008). Experimental evidence supports this hypothesis, showing

Table 1
Descriptive statistics of number of included cities, cumulative confirmed COVID-19 cases ($n = 95,175,005$), environmental exposures, governmental stringency index, and vaccination coverage in the different countries.

Country	Number of included cities	COVID-19 cases	Daily mean humidex Mean (range) [°C]	Daily mean $PM_{2.5}$ Mean (range) [μg/m^3]	Daily mean ultraviolet solar radiation Mean (range) [J/m^2]	Daily mean precipitation Mean (range) [mm]	Daily mean OxCGRT GSI Mean (range) [%]	Daily mean vaccination coverage Mean (range) [%]
Australia	1	163,026	23.7 (9.2, 39.1)	6.4 (2.4, 23.8)	187.5 (14.2, 366.6)	3.6 (0.0, 155.7)	55.8 (11.1, 78.2)	29.6 (0.0, 82.7)
Brazil	18	4,651,427	31.4 (1.2, 42.5)	15.2 (3.1, 140.6)	209.6 (7.8, 381.1)	3.9 (0.0, 189.8)	56.2 (11.1, 81.0)	28.6 (0.0, 79.4)
Canada	3	474,377	5.1 (–39.6, 37.8)	26.5 (2.0, 119.9)	163.1 (2.6, 365.6)	3.3 (0.0, 91.1)	61.0 (2.8, 76.4)	34.5 (0.0, 81.9)
Chile	3	286,717	13.4 (–2.1, 27.2)	41.1 (4.8, 242.6)	209.0 (3.9, 413.0)	1.9 (0.0, 59.9)	62.0 (25.6, 90.3)	42.3 (0.0, 90.0)
Czech Republic	1	528,084	10.5 (–17.3, 30.3)	13.6 (1.8, 56.1)	148.0 (6.7, 327.3)	2.2 (0.0, 83.3)	46.4 (11.1, 82.4)	29.2 (0.0, 65.6)
Estonia	1	283,494	7.2 (–21.7, 32.6)	6.7 (2.3, 22.7)	132.1 (1.9, 334.7)	2.0 (0.0, 39.9)	37.9 (0.0, 77.8)	28.9 (0.0, 64.6)
Germany	11	4,469,697	11.3 (–17.3, 33.8)	10.8 (1.3, 58.6)	143.5 (2.5, 339.5)	2.3 (0.0, 91.2)	54.0 (14.8, 85.2)	33.4 (0.0, 76.1)
Italy	23	9,125,657	18.0 (–9.4, 40.7)	13.0 (2.0, 109.4)	191.7 (5.3, 348.3)	2.2 (0.0, 84.0)	60.2 (19.2, 93.5)	35.5 (0.0, 81.2)
Japan	10	9,262,517	18.3 (–18.1, 44.0)	17.3 (4.2, 93.6)	169.6 (10.3, 344.7)	4.7 (0.0, 184.8)	43.4 (25.9, 55.1)	33.0 (0.0, 82.8)
Kuwait	1	707,652	30.2 (4.7, 51.4)	37.9 (14.8, 62.7)	237.7 (27.2, 335.4)	0.2 (0.0, 29.4)	59.1 (11.1, 100.0)	30.7 (0.0, 78.0)
Mexico	11	3,668,658	19.3 (–10.1, 38.4)	20.6 (2.4, 129.4)	258.4 (28.7, 384.5)	1.7 (0.0, 106.2)	51.8 (2.8, 82.4)	23.8 (0.0, 62.7)
Netherland	5	1,133,885	12.3 (–12.5, 33.7)	10.8 (2.5, 80.4)	145.3 (3.5, 333.5)	2.3 (0.0, 38.3)	51.1 (15.7, 82.4)	31.1 (0.0, 68.1)
Norway	1	197,392	6.9 (–20.5, 27.6)	7.1 (2.1, 40.6)	128.0 (1.0, 340.2)	2.5 (0.0, 37.9)	41.6 (11.1, 79.6)	33.0 (0.0, 74.5)
Peru	18	3,264,402	17.1 (–3.1, 40.6)	33.2 (2.6, 123.1)	235.5 (34.8, 400.9)	3.7 (0.0, 106.1)	69.2 (13.9, 96.3)	27.0 (0.0, 82.2)
Philippines	4	505,630	37.4 (28.0, 43.4)	13.8 (5.3, 46.9)	201.7 (21.5, 317.2)	6.7 (0.0, 186.7)	67.3 (26.6, 100.0)	18.0 (0.0, 62.2)
Romania	8	1,367,362	12.2 (–17.8, 37.1)	17.4 (5.2, 83.0)	163.0 (4.2, 338.2)	1.8 (0.0, 45.4)	52.2 (11.1, 87.0)	17.3 (0.0, 41.3)
Singapore	1	1,817,744	38.1 (33.5, 41.1)	NA	190.2 (26.9, 296.1)	7.4 (0.0, 90.8)	49.4 (25.0, 82.4)	40.0 (0.0, 90.2)
South Africa	1	414,972	18.3 (7.7, 31.4)	27.4 (8.0, 206.5)	202.8 (19.0, 396.6)	1.6 (0.0, 37.7)	52.3 (11.1, 88.0)	10.7 (0.0, 32.1)
Spain	52	10,453,752	16.1 (–9.0, 39.4)	10.7 (1.6, 296.5)	189.8 (5.5, 368.6)	1.8 (0.0, 77.0)	58.1 (35.4, 85.2)	29.6 (0.0, 84.6)
Switzerland	8	2,399,955	10.8 (–14.3, 34.7)	10.8 (1.4, 59.5)	165.5 (3.4, 352.2)	3.7 (0.0, 80.6)	42.0 (11.1, 73.2)	31.2 (0.0, 68.7)
United Kingdom	54	7,426,224	11.1 (–8.3, 32.4)	11.4 (1.9, 82.2)	131.5 (1.2, 351.2)	2.4 (0.0, 48.3)	53.5 (11.1, 88.0)	34.7 (0.0, 74.3)
United States	204	32,572,370	16.0 (–35.5, 44.9)	10.3 (0.9, 413.0)	189.5 (2.2, 385.1)	2.9 (0.0, 246.0)	57.9 (20.4, 75.5)	28.0 (0.0, 81.5)

Abbreviations: COVID-19, coronavirus disease 2019; $PM_{2.5}$, fine particulate matter ≤ 2.5 μm; OxCGRT GSI, Oxford COVID-19 Government Response Tracker Government Stringency Index; NA, not available.

that the virus remains stable at approximately 4 °C, whereas exposure to 70 °C inactivates the virus within 5 min (Chin et al., 2020). From the host's perspective, inhalation of cold, dry air can cool the nasal epithelium, impairing key respiratory defenses such as mucociliary clearance (Kudo et al., 2019). Animal studies suggest that low temperatures can suppress local immune responses, including reduced activity of virus-specific $CD8^+$ T cells and lower IgG antibody production, likely due to diminished mucosal circulation and compromised adaptive immunity(Moriyama and Ichinohe, 2019). Low humidity may also increase airborne transmission risk by accelerating droplet evaporation and promoting the formation of smaller droplet nuclei that remain suspended for longer periods (Rosti et al., 2020; Wei et al., 2022). Behavioral factors contribute as well, since cold, dry weather often leads to increased time spent indoors in enclosed or poorly ventilated spaces, facilitating viral spread through closer interpersonal contact and limited air exchange (Fares, 2013). Collectively, these mechanisms highlight the need to integrate epidemiological, experimental, and behavioral evidence to better understand climate-related pathways in COVID-19 transmission. Our global finding that lower humidex is associated with higher COVID-19 incidence is consistent with these mechanistic pathways.

Our findings suggest a positive association between short-term exposure to $PM_{2.5}$ and the risk of COVID-19 infection on a global scale, consistent with earlier epidemiological evidence, including multicenter studies and *meta*-analyses described in the introduction (Kim et al., 2022; Stafoggia et al., 2023; Wu et al., 2020;Yu et al., 2024; Zhu et al., 2020). This association is further supported by a nationwide cohort study in Denmark, which reported a significant positive relationship between $PM_{2.5}$ exposure and COVID-19 infection risk, and by a large-scale cohort study in China linking long-term $PM_{2.5}$ exposure with elevated risks of long COVID, hospitalization, and lower levels of SARS-CoV-2-specific IgG antibodies (Yan et al., 2025; J. Zhang et al., 2023). Evidence on the role of air pollutants in facilitating COVID-19 transmission remains limited, primarily due to the scarcity of comprehensive population-based studies. Several plausible biological mechanisms have been proposed, including the potential for PM to act as an environmental carrier, promoting the airborne transport and inhalation of viral particles into the respiratory tract (Martelletti and Martelletti, 2020). Air

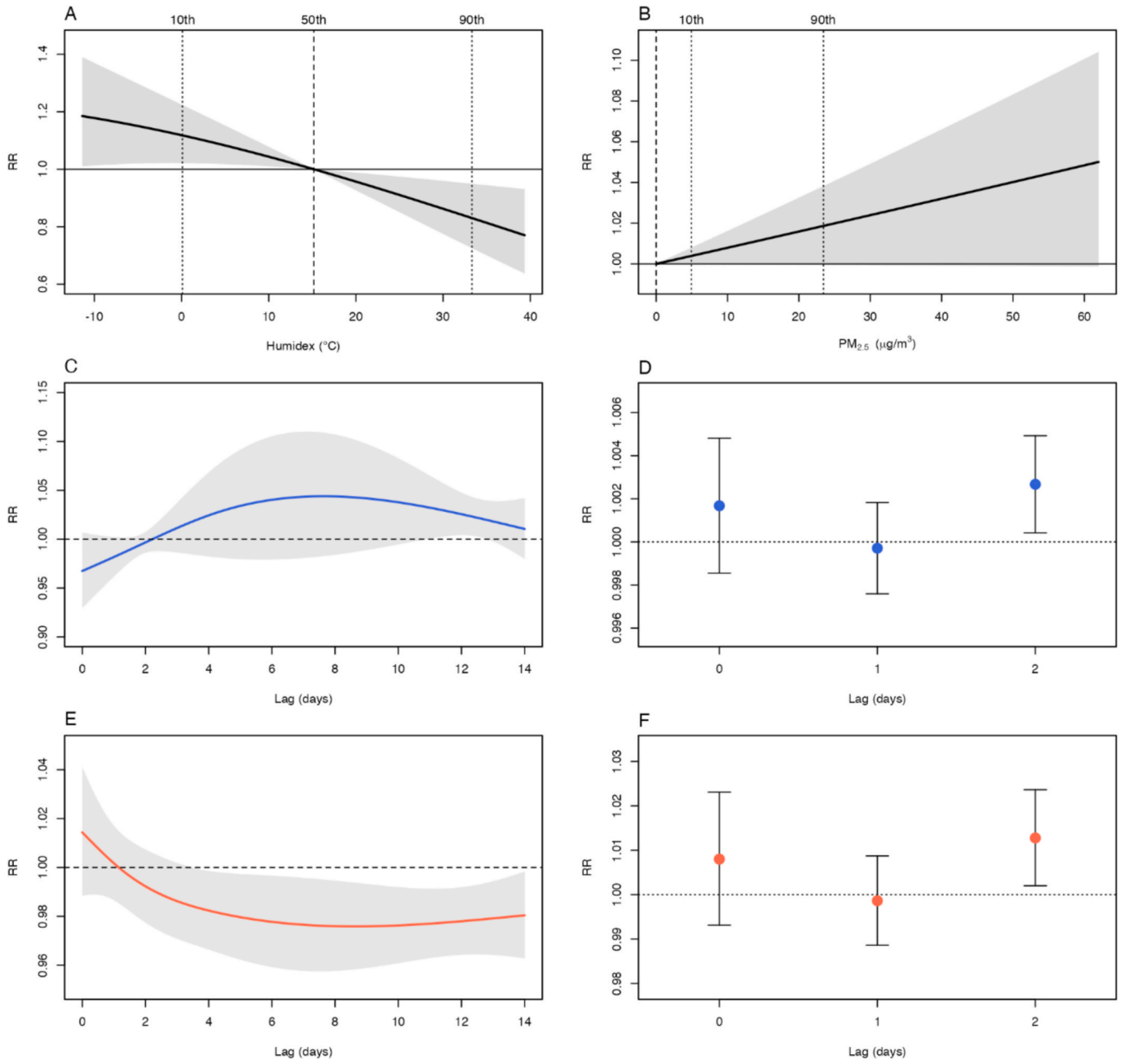

Fig. 3. Overall cumulative exposure–response relationships and lag–response relationships between humidex, $PM_{2.5}$ concentration, and COVID-19 incidence with 95% CIs. Notes: In Panel A, vertical lines represent the 10^{th}, 50^{th} (median), and 90^{th} percentiles of the humidex distribution. The y-axis depicts the overall cumulative RR of daily COVID-19 cases in humidex, centered at the median. In Panel B, vertical lines correspond to 0 μg/m^3 as well as the 10^{th} and 90^{th} percentiles of the $PM_{2.5}$ distribution. The y-axis shows the overall cumulative RR per 10 μg/m^3 increase in $PM_{2.5}$, centered at 0 μg/m^3. Panels C and D illustrate the cumulative RR at the 10^{th} percentile of humidex (Panel C) and $PM_{2.5}$ (Panel D), respectively. Panels E and F likewise present the cumulative RR at the 90^{th} percentile of humidex (Panel E) and $PM_{2.5}$ (Panel F). Abbreviations: $PM_{2.5}$, fine particulate matter $\leq$ 2.5 μm; COVID-19, coronavirus disease 2019; RR, relative risk; CI, confidence interval.

pollution is thought to impair host defense mechanisms through multiple pathways, including disruption of epithelial barriers, dysregulation of alveolar macrophage activity, perturbations of the respiratory microbiome, and upregulation of cellular receptors that facilitate viral entry (Monoson et al., 2023). Additionally, exposure to $PM_{2.5}$ has been shown to dysregulation the immune system, characterized by overexpression of pro-inflammatory cytokines and chemokines (Lavigne et al., 2023). These immune disturbances may trigger inappropriate local and systemic inflammatory responses, increasing susceptibility to SARS-CoV-2 infection and accelerating disease progression. Moreover, immune dysfunction may lower the host threshold for secondary or opportunistic infections and exacerbate pre-existing non-infectious conditions such as asthma, further compromising outcomes in COVID-19 patients (Madaniyazi and Xerxes, 2021). Emerging experimental evidence has elucidated molecular mechanisms underlying these observations. Animal studies have shown $PM_{2.5}$ exposure upregulates angiotensin-converting enzyme 2 (ACE2), the primary receptor SARS-CoV-2, thereby enhancing viral entry and replication in both *in vitro* and *in vivo* systems (Lin et al., 2025; Scialo et al., 2020). These findings provide mechanistic support for the hypothesis that ambient $PM_{2.5}$ exposure may increase susceptibility to SARS-CoV-2 infection and contribute to more severe clinical trajectories. Consistent with this, our analysis revealed a positive association between the $PM_{2.5}$ exposure and COVID-19 incidence, albeit under a specific lag structure and with

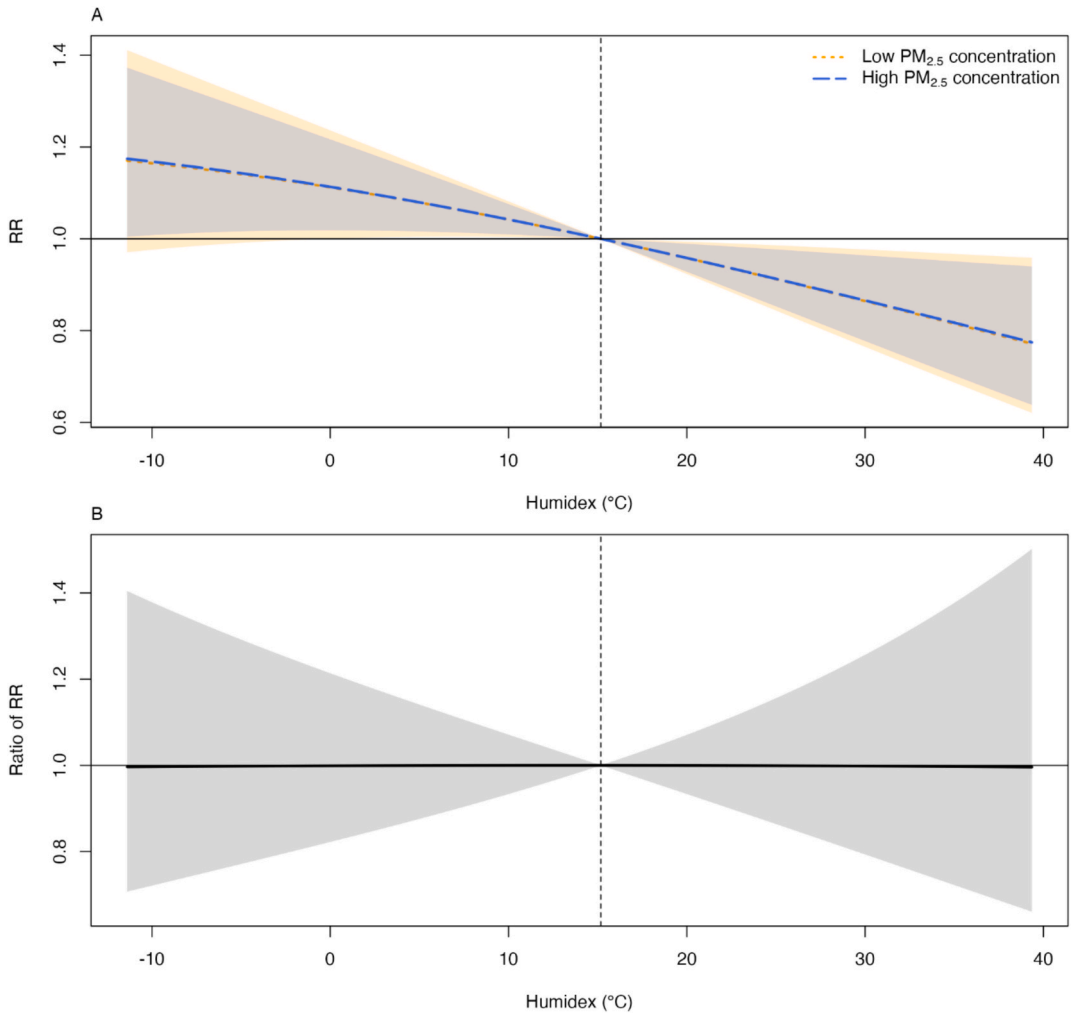

Fig. 4. Overall cumulative exposure–response relationships between humidex and COVID-19 incidence by $PM_{2.5}$ concentration with 95% CIs. Notes: Panel A illustrates the RRs for the overall cumulative exposure–response relationship between humidex and COVID-19 incidence, estimated at low (10^{th} percentile; solid light-orange lines) and high (90^{th} percentile; dashed light-purple lines) $PM_{2.5}$ concentrations, with 95% CIs depicted by shaded areas. Panel B presents the interaction between $PM_{2.5}$ concentration and the overall cumulative humidex–COVID-19 association, expressed as the ratio of RRs at the 10^{th} and 90^{th} $PM_{2.5}$ percentiles, with corresponding 95% CIs likewise shown as shaded regions. Vertical line marks the 50^{th} (median) percentile of the humidex distribution. Abbreviations: $PM_{2.5}$, fine particulate matter $\leq$ 2.5 μm; COVID-19, coronavirus disease 2019; RR, relative risk; CI, confidence interval. (For interpretation of the references to colour in this figure legend, the reader is referred to the web version of this article.)

relatively wide CIs. Overall, it seems that the association is stronger within a short lag period, suggesting that $PM_{2.5}$ could be implicated in the development of the symptoms after infection. This pattern may reflect an acute triggering effect, however the findings should be interpreted cautiously due to potential delays between exposure, symptom onset, and case reporting. Further studies are warranted to validate the relationship between ambient air pollution and COVID-19 incidence. Within this growing body of research, our analysis provides multi-country, time-series evidence that short-term increases in $PM_{2.5}$ are associated with small but measurable increases in COVID-19 incidence.

To the best of our knowledge, this is the first global study to investigate the interactive effects of $PM_{2.5}$ concentrations on the association between humidex and COVID-19 incidence. We observed no significant effect of $PM_{2.5}$, providing no empirical support for the prevailing hypothesis that air pollution amplifies the health impacts of meteorological stressors on COVID-19 incidence. This finding contrasts with a regional study from Belgium, the only prior study examining this interaction which reported that elevated $PM_{2.5}$ levels modified the temperature–COVID-19 relationship, heightening infection risk under both cold and hot conditions (Thi Khanh et al., 2024). From a mechanistic standpoint, several pathways have been proposed to explain the potential synergy between air pollutants and thermal stress. For instance, low-humidity environments may impair the dispersion of air pollutants and reduce mucociliary clearance, thereby increasing pulmonary exposure to inhaled particulates (Ma et al., 2016). In colder settings, elevated fossil fuel combustion can further raise ambient pollutant concentrations. Despite the plausibility of these mechanisms, the absence of detectable interactions in this study may be attributed to several factors. First, $PM_{2.5}$ levels during the study period may not have been sufficiently high to elicit synergistic effects with meteorological exposures. Notably, $PM_{2.5}$ concentrations declined markedly during the COVID-19 lockdowns, with an average reduction of 31.0% reported across 34 countries (Venter et al., 2020). Recent time-series studies have also documented significant improvements in air quality and corresponding reductions in mortality during the early lockdown period of 2020 in Jiangsu (China), California (United States), central-southern Italy, and Germany (Ma et al., 2024). Second, behavioral adaptations during the pandemic, such as widespread mask use, improved ventilation, and reduced outdoor activity, may have mitigated actual exposure to both environmental stressors (Bollyky et al., 2023). Third, variability in $PM_{2.5}$ composition across locations, combined with the limited in temporal and spatial resolution of exposure metrics, could have further

attenuated the ability to detect effect modification (Manchanda et al., 2021). While several studies have linked $PM_{2.5}$ concentrations with increased COVID-19 incidence, research evaluating its role as an effect modifier in the context of environmental co-exposures remain scarce. Further studies are warranted to clarify the underlying biological and behavioral mechanisms, investigate differential susceptibility, and examine these associations in diverse climatic and pollution contexts, including analyses using individual-level exposure data and studies conducted in regions with high pollution burdens. Taken together, our findings suggest that, within the exposure ranges observed during the study period, $PM_{2.5}$ primarily acts as an independent risk factor rather than a modifier of the humidex–COVID-19 relationship.

This study has several notable strengths. First, it encompassed 439 cities across 22 countries, covering a wide range of humidex and $PM_{2.5}$ levels across both warm and cold seasons. The use of comprehensive, standardized, and state-of-the-art statistical protocols ensures methodological consistency, thereby enabling valid cross-location comparisons and minimizing heterogeneity. In particular, we adopted an extended two-stage design combining city-specific quasi-Poisson regression with DLNMs and multilevel random-effects *meta*-regression, a framework that has been widely applied in environmental epidemiology to derive comparable exposure–lag–response associations across locations (Sera and Gasparrini, 2022). The inclusion of distributed lag terms for government stringency and vaccination coverage, together with autoregressive terms for lagged case counts, further strengthened control of time-varying confounding and underlying transmission dynamics. To the best of our knowledge, this represents the most extensive investigation of its kind to date. The large sample size provided substantial statistical power and robustness to the analysis. Specifically, the dataset included nearly 95 million confirmed COVID-19 cases, accounting for approximately 16.0% of the six billion global cases recorded as of 31 August 2022 (Feurer et al., 2024). Second, the observational period was considerably longer than that of most previous COVID-19 studies. By spanning 2.5 years, the study captured multiple waves of infection across distinct pandemic phases, each characterized by varying dominant variants and vaccination coverage. To the best of our knowledge, few previous studies have analyzed such a large number of locations at this fine spatial resolution or over such an extended period to investigate multiple environmental exposures in relation to COVID-19 incidence. This study represents the first global analysis to provide detailed evidence on the short-term effects of humidex and $PM_{2.5}$ concentrations, as well as their potential interaction. Furthermore, comprehensive sensitivity analyses consistently supported the main findings, reinforcing the robustness and reliability of the results.

However, this study has some limitations. First, although the dataset includes a large number of cities, it does not fully represent the global population. Substantial geographical gaps remain: Latin America, Southeast Asia, and Oceania are only modestly represented, whereas Northern and Central Africa, the Middle East, and much of Central and Northern Asia are entirely absent. Even in regions with relatively high coverage, some countries contributed data from only one or a few cities. Furthermore, the dataset is based on urban locations whereas rural areas have different population structures, healthcare systems, and air pollution patterns. Therefore, the findings should be interpreted as reflective of the 439 included cities rather than broadly generalizable to the 22 participating countries or the global population. Second, as an ecological study, uniform exposure was assumed across cities on a given day. Exposure estimates were based on averages from a limited number of monitoring sites, which may not capture within-city variability and could introduce measurement errors. Third, gridded exposure data were used as proxies for individual-level exposure, potentially resulting in exposure misclassification. For instance, $PM_{2.5}$ concentrations were estimated using model-based approaches rather than ground-based monitoring. In some locations (i.e., Maceió, Recife, São Luís, Lima, and Singapore), $PM_{2.5}$ data did not cover the whole study period due to missing values (Table S2). Future studies should assess the consistency of exposure–response estimates based on modeled versus observed air quality data, particularly in the post-pandemic period (W. Yu et al., 2024a). Fourth, effect estimates ate at low humidex values should be interpreted with caution as readings below < 20 °C fall outside widely recognized heat-stress ranges and may not accurately reflect levels of humid-heat discomfort (CCOHS, 2025). Although humidex pragmatically combines temperature and humidity, it omits wind speed, radiative load, and cloud cover. Consequently, physiologically grounded indices, such as the WBGT and UTCI, may better characterize thermal stress and should be evaluated in future analyses. Fifth, due to limited data availability, we were unable to assess the short-term effects of other air pollutants, such as PM_{10}, CO, NO_2, and O_3, on COVID-19 incidence, or to evaluate potential confounding effects of co-exposure through bi- or multi-pollutant models. Sixth, variations in the definitions of confirmed cases and reporting protocols across countries may have introduced systematic differences in surveillance data. Moreover, the OxCGRT GSI, constructed at the national level, may not have captured subnational variations in policy interventions, thereby limiting its ability to reflect local heterogeneity in response measures and leaving some residual confounding by local mitigation policies. This limitation could have biased the estimated short-term associations between environmental exposures and COVID-19 incidence in either direction and may partly account for the substantial between-city heterogeneity observed in our *meta*-analyses. Seventh, although this study provides global estimates, their interpretation should be made with caution given the substantial heterogeneity across locations (i.e., $I^2 = 75.5\%$ for humidex and $I^2 = 64.6\%$ for $PM_{2.5}$). Eighth, our analyses were restricted to January 2020–August 2022, corresponding to the period for which harmonized high-quality multi-country, city-level data were available. Subsequent phases of the pandemic have been characterized by changes in dominant variants, vaccination coverage, population immunity, and case-ascertainment practices, which may influence both baseline risks and the magnitude of environmental associations. Future research should extend these analyses with more recent data where feasible and systematically explore this spatial and temporal heterogeneity to identify potential modifiers such as vaccination coverage, OxCGRT GSI, and socioeconomic and demographic factors. Ninth, the daily COVID-19 case counts used in our analyses were based on confirmation or reporting dates in routine surveillance systems, rather than on the underlying dates of infection. In general, delays from infection to symptom onset, testing, and reporting, likely to vary across countries and over time, introduce uncertainty in the temporal alignment between environmental exposures and case occurrence. This complicates a mechanistic interpretation of the distributed lag structure and may blur or shift the estimated lag patterns, as well as contribute to the between-city heterogeneity observed in our *meta*-analyses. Future studies combining environmental data with individual-level information on symptom onset or infection times would help refine the timing of the exposure–response relationships. Finally, although the extended two-stage design allowed us to flexibly model complex exposure–lag–response associations, the results inevitably depend on modelling choices; we explored these choices through extensive sensitivity analyses, but some degree of model misspecification and residual confounding cannot be entirely excluded.

5. Conclusions

This multi-country time-series study provides global evidence on the independent effects of humidex and $PM_{2.5}$ on daily COVID-19 incidence during the first 2.5 years of the pandemic. Overall, short-term exposure to lower humidex values and elevated $PM_{2.5}$ concentrations was associated with an increased number of COVID-19 cases. Additionally, $PM_{2.5}$ exposure did not significantly modify the humidex–COVID-19 association. These finding enhance our understanding of the complex interplay between meteorology, air quality, and the infectious disease transmission, offering valuable insights for designing targeted public health interventions, strengthening health systems, and planning climate-

resilient cities, and provide a foundation for future studies that reassess environmental early warning tools using post-2022 data under endemic conditions.

8. Data sharing statement

Data were collected within the MCC Collaborative Research Network (https://mccstudy.lshtm.ac.uk/) under a data-sharing agreement and could not be made publicly available. Upon reasonable request, researchers can refer to the corresponding authors for data access and the R code used in the analyses.

CRediT authorship contribution statement

Keita Wagatsuma: Writing – review & editing, Writing – original draft, Validation, Methodology, Funding acquisition, Formal analysis, Data curation, Conceptualization. **Denise Feurer:** Writing – review & editing, Methodology. **Wenhua Yu:** Writing – review & editing, Data curation. **Rongbin Xu:** Writing – review & editing, Data curation. **Tim Riffe:** Writing – review & editing, Data curation. **Maxi Stella Kniffka:** Writing – review & editing, Data curation. **Enrique Acosta:** Writing – review & editing, Data curation. **Ben Armstrong:** Writing – review & editing, Data curation. **Malcolm Mistry:** Writing – review & editing, Data curation. **Rachel Lowe:** Writing – review & editing, Funding acquisition, Data curation. **Dominic Royé:** Writing – review & editing, Funding acquisition, Data curation. **Masahiro Hashizume:** Writing – review & editing, Data curation. **Aurelio Tobias:** Writing – review & editing, Data curation. **Ana Maria Vicedo-Cabrera:** Writing – review & editing, Funding acquisition, Data curation. **Lina Madaniyazi:** Writing – review & editing, Data curation. **Chris Fook Sheng Ng:** Writing – review & editing, Data curation. **Carmen Íñiguez:** Writing – review & editing, Data curation. **Martina S. Ragettli:** Writing – review & editing, Data curation. **Eric Lavigne:** Writing – review & editing, Data curation. **Patricia Matus Correa:** Writing – review & editing, Data curation. **Nicolás Valdés Ortega:** Writing – review & editing, Data curation. **Jan Kyselý:** Writing – review & editing, Funding acquisition, Data curation. **Aleš Urban:** Writing – review & editing, Funding acquisition, Data curation. **Hans Orru:** Writing – review & editing, Data curation. **Ene Indermitte:** Writing – review & editing, Data curation. **Marek Maasikmets:** Writing – review & editing, Data curation. **Susanne Breitner-Busch:** Writing – review & editing, Data curation. **Alexandra Schneider:** Writing – review & editing, Data curation. **Yasushi Honda:** Writing – review & editing, Data curation. **Barrak Alahmad:** Writing – review & editing, Data curation. **Antonella Zanobetti:** Writing – review & editing, Data curation. **Joel Schwartz:** Writing – review & editing, Data curation. **Gabriela Carrasco:** Writing – review & editing, Data curation. **Iulian Horia Holobâca:** Writing – review & editing, Data curation. **Ho Kim:** Writing – review & editing, Data curation. **Whanhee Lee:** Writing – review & editing, Data curation. **Michelle L. Bell:** Writing – review & editing, Data curation. **Noah Scovronick:** Writing – review & editing, Data curation. **Fiorella Acquaotta:** Writing – review & editing, Data curation. **Micheline de Sousa Zanotti Stagliorio Coelho:** Writing – review & editing, Data curation. **Magali Hurtado Diaz:** Writing – review & editing, Data curation. **Eunice Elizabeth Félix Arellano:** Writing – review & editing, Data curation. **Paola Michelozzi:** Writing – review & editing, Data curation. **Massimo Stafoggia:** Writing – review & editing, Data curation. **Francesca de'Donato:** Writing – review & editing, Data curation. **Shilpa Rao:** Writing – review & editing, Data curation. **Xerxes Seposo:** Writing – review & editing, Data curation. **Shilu Tong:** Writing – review & editing, Data curation. **Jochem Klompmaker:** Writing – review & editing, Data curation. **Yuming Guo:** Writing – review & editing, Data curation. **Pierre Masselot:** Writing – review & editing, Data curation. **Antonio Gasparrini:** Writing – review & editing, Data curation. **Francesco Sera:** Writing – review & editing, Writing – original draft, Supervision, Methodology, Funding acquisition, Data curation, Conceptualization.

6. Ethics approval and consent to participate

Because all data used in the present study were aggregated, anonymized, and obtained from publicly accessible sources and the MCC Collaborative Research Network, ethical approval was not required.

Consent for publication

Not applicable.

Funding

K.W. was supported by the Japan Society for the Promotion of Science (Grant Nos. 24 K23680 and 25 K20622). D.F. acknowledges funding from the European Union—Next Generation EU through the project of national interest (PRIN) "Geo-Intelligence for improved air quality monitoring and analysis (GeoAIr)" (Grant No. 202258ACSL). R. L. acknowledges support from the Royal Society (Hodgkin Fellowship) and the European Union's Horizon Europe Research and Innovation Program (Grant No. 101057554, project IDAlert, https://idalertproject.eu). The IDAlert is part of the EU Climate Change and Health Cluster (https://climate-health.eu). D.R. is supported by a 'Ramón y Cajal' fellowship program of the Spanish Ministry of Science and Innovation (Grant No. RYC2023-042824-I). A.M.V.C. received support from the Swiss National Science Foundation (Grant No. TMSGI3_211626). J.K. and A.U. received support from the Czech Science Foundation (Grant No. 25-17587S). F.S. received funding from the Italian Ministry of University and Research under the Department of Excellence project 2023–2027 "ReDS – Rethinking Data Science," Department of Statistics, Computer Science and Applications, University of Florence. The funders played no role in the study design, data collection, data analysis, data interpretation, or manuscript writing.

Declaration of competing interest

The authors declare that they have no known competing financial interests or personal relationships that could have appeared to influence the work reported in this paper.

Acknowledgment

We acknowledge the contributions and support of all authors of this paper.

Appendix A. Supplementary data

Supplementary data to this article can be found online at https://doi.org/10.1016/j.envint.2026.110090.

Data availability

The data that has been used is confidential.

References

Armstrong, B., Sera, F., Vicedo-Cabrera, A.M., Abrutzky, R., Åström, D.O., Bell, M.L., Chen, B.Y., Coelho, M.de.S.Z.S., Correa, P.M., Dang, T.N., Diaz, M.H., Van Dung, D., Forsberg, B., Goodman, P., Guo, Y.L.L., Guo, Y., Hashizume, M., Honda, Y., Indermitte, E., Íñiguez, C., Kan, H., Kim, H., Kyselý, J., Lavigne, E., Michelozzi, P., Orru, H., Ortega, N.V., Pascal, M., Ragettli, M.S., Saldiva, P.H.N., Schwartz, J., Scortichini, M., Seposo, X., Tobias, A., Tong, S., Urban, A., Valencia, C.D.la.C., Zanobetti, A., Zeka, A., Gasparrini, A., 2019. The role of humidity in associations of high temperature with mortality: a multicountry, multicity study. Environ. Health Perspect. 127, 097007. https://doi.org/10.1289/EHP5430.

Bherwani, H., Nair, M., Musugu, K., Gautam, S., Gupta, A., Kapley, A., Kumar, R., 2020. Valuation of air pollution externalities: comparative assessment of economic damage and emission reduction under COVID-19 lockdown. Air Qual. Atmos. Health 13, 683–694. https://doi.org/10.1007/s11869-020-00845-3.

Bherwani, H., Anjum, S., Kumar, S., Gautam, S., Gupta, A., Kumbhare, H., Anshul, A., Kumar, R., 2021. Understanding COVID-19 transmission through Bayesian probabilistic modeling and GIS-based Voronoi approach: a policy perspective.

Environ. Dev. Sustain. 23, 5846–5864. https://doi.org/10.1007/s10668-020-00849-0.
Bollyky, T.J., Castro, E., Aravkin, A.Y., Bhangdia, K., Dalos, J., Hulland, E.N., Kiernan, S., Lastuka, A., McHugh, T.A., Ostroff, S.M., Zheng, P., Chaudhry, H.T., Ruggiero, E., Turilli, I., Adolph, C., Amlag, J.O., Bang-Jensen, B., Barber, R.M., Carter, A., Chang, C., Cogen, R.M., Collins, J.K., Dai, X., Dangel, W.J., Dapper, C., Deen, A., Eastus, A., Erickson, M., Fedosseeva, T., Flaxman, A.D., Fullman, N., Giles, J.R., Guo, G., Hay, S.I., He, J., Helak, M., Huntley, B.M., Iannucci, V.C., Kinzel, K.E., LeGrand, K.E., Magistro, B., Mokdad, A.H., Nassereldine, H., Ozten, Y., Pasovic, M., Pigott, D.M., Reiner, R.C., Reinke, G., Schumacher, A.E., Serieux, E., Spurlock, E.E., Troeger, C.E., Vo, A.T., Vos, T., Walcott, R., Yazdani, S., Murray, C.J.L., Dieleman, J. L., 2023. Assessing COVID-19 pandemic policies and behaviours and their economic and educational trade-offs across US states from Jan 1, 2020, to July 31, 2022: an observational analysis. Lancet 401, 1341–1360. https://doi.org/10.1016/S0140-6736(23)00461-0.
Briz-Redón, Á., Serrano-Aroca, Á., 2020. The effect of climate on the spread of the COVID-19 pandemic: a review of findings, and statistical and modelling techniques. Prog. Phys. Geogr. 44, 591–604. https://doi.org/10.1177/0309133320946302.
CCOHS, 2025. Humidex Rating and Work. Available from: https://www.ccohs.ca/oshanswers/phys_agents/humidex.html. (Accessed 6 September 2025)., n.d.
Chakraborty, C., Bhattacharya, M., Chatterjee, S., Lee, S.-S., Bhattacharya, P., Ohimain, E.I., Wen, Z.-H., Das, A., Rai, A., Abdelhameed, A.S., Agoramoorthy, G., Zayed, H., Byrareddy, S.N., 2025. Comprehensive global-scale evaluation of the COVID-19 pandemic associated with 234 countries, territories, and sub-national locations during 2020–2024. Folia Microbiol. (Praha) 1–31. https://doi.org/10.1007/s12223-025-01299-9.
Chan, K.H., Peiris, J.S.M., Lam, S.Y., Poon, L.L.M., Yuen, K.Y., Seto, W.H., 2011. The effects of temperature and relative humidity on the viability of the SARS coronavirus. Adv. Virol. 1, 734690. https://doi.org/10.1155/2011/734690.
Cheuvront, S.N., Caruso, E.M., Heavens, K.R., Karis, A.J., Santee, W.R., Troyanos, C., D'Hemecourt, P., 2015. Effect of WBGT index measurement location on heat stress category classification. Med. Sci. Sports Exerc. 47, 1958–1964. https://doi.org/10.1249/MSS.0000000000000624.
Chin, A.W.H., Chu, J.T.S., Perera, M.R.A., Hui, K.P.Y., Yen, H.L., Chan, M.C.W., Peiris, M., Poon, L.L.M., 2020. Stability of SARS-CoV-2 in different environmental conditions. Lancet Microbe. https://doi.org/10.1016/S2666-5247(20)30003-3.
Chong, K.C., Zhao, S., Hung, C.T., Jia, K.M., Ho, J.Y.en., Lam, H.C.Y., Jiang, X., Li, C., Lin, G., Yam, C.H.K., Chow, T.Y., Wang, Y., Li, K., Wang, H., Wei, Y., Guo, Z., Yeoh, E.K., 2024. Association between meteorological variations and the superspreading potential of SARS-CoV-2 infections. Environ. Int. 188, 108762. https://doi.org/10.1016/j.envint.2024.108762.
d'Ambrosio Alfano, F.R., Palella, B.I., Riccio, G., 2011. Thermal environment assessment reliability using temperature -Humidity indices. Ind. Health 49, 95–106. https://doi.org/10.2486/indhealth.MS1097.
Donzelli, G., Biggeri, A., Tobias, A., Nottmeyer, L.N., Sera, F., 2022. Role of meteorological factors on SARS-CoV-2 infection incidence in Italy and Spain before the vaccination campaign. a multi-city time series study. Environ. Res. 211, 113134. https://doi.org/10.1016/j.envres.2022.113134.
Fan, C., Liu, F., Zhao, X., Ma, Y., Yang, F., Chang, Z., Xiao, X., 2020. An alternative comprehensive index to quantify the interactive effect of temperature and relative humidity on hand, foot and mouth disease: a two-stage time series study including 143 cities in mainland China. Sci. Total Environ. 740, 140106. https://doi.org/10.1016/j.scitotenv.2020.140106.
Fares, A., 2013. Factors influencing the seasonal patterns of infectious diseases. Int. J. Prev. Med. 4, 128.
Feurer, D., Riffe, T., Kniffka, M.S., Acosta, E., Armstrong, B., Mistry, M., Lowe, R., Royé, D., Hashizume, M., Madaniyazi, L., Ng, C.F.S., Tobias, A., Íñiguez, C., Vicedo-Cabrera, A.M., Ragettli, M.S., Lavigne, E., Correa, P.M., Ortega, N.V., Kyselý, J., Urban, A., Orru, H., Indermitte, E., Maasikmets, M., Dallavalle, M., Schneider, A., Honda, Y., Alahmad, B., Zanobetti, A., Schwartz, J., Carrasco, G., Holobâca, I.H., Kim, H., Lee, W., Bell, M.L., Scovronick, N., Acquaotta, F., Coélho, M.de.S.Z.S., Diaz, M.H., Arellano, E.E.F., Michelozzi, P., Stafoggia, M., de'Donato, F., Rao, S., Di Ruscio, F., Seposo, X., Guo, Y., Tong, S., Masselot, P., Gasparrini, A., Sera, F., 2024. Meteorological factors, population immunity, and COVID-19 incidence a global multi-city analysis. Environ. Epidemiol. 8, e338.
Ford, J.D., Zavaleta-Cortijo, C., Ainembabazi, T., Anza-Ramirez, C., Arotoma-Rojas, I., Bezerra, J., Chicmana-Zapata, V., Galappaththi, E.K., Hangula, M., Kazaana, C., Lwasa, S., Namanya, D., Nkwinti, N., Nuwagira, R., Okware, S., Osipova, M., Pickering, K., Singh, C., Berrang-Ford, L., Hyams, K., Miranda, J.J., Naylor, A., New, M., van Bavel, B., Angula, M., Arvind, J., Akugre, F.A., Bazaz, A., Coggins, S., Crowley, F., Dharmasiri, I.P., Fernandez-de-Larrinoa, Y., George, B., Harper, S., Jones, B., Jones, G., Jones, K., Kaur, H., Krishnakumar, J., Kunamwene, I., Mangalasseri, A., Mcguire, C., Mensah, A., Nkalubo, J., Pearce, T., Perera, C.D., Poonacha Kodira, P., Scanlon, H., Togarepi, C., Varghese, A., Wright, C., 2022. Interactions between climate and COVID-19. Lancet Planet Health. 6, e825–e833. https://doi.org/10.1016/S2542-5196(22)00174-7.
Gao, Q., Jiang, B., Tong, M., Zuo, H., Cheng, C., Zhang, Y., Song, S., Lu, L., Li, X., 2025. Effects and interaction of humidex and air pollution on influenza: a national analysis of 319 cities in mainland China. J. Hazard. Mater. 490, 137865. https://doi.org/10.1016/j.jhazmat.2025.137865.
Gasparrini, A., 2011. Distributed lag linear and non-linear models in R: the package dlnm. J. Stat. Softw. 43, 1–20. https://doi.org/10.18637/jss.v043.i08.
Gasparrini, A., Vicedo-Cabrera, A.M., Tobias, A., 2024. The Multi-Country Multi-City Collaborative Research Network: an international research consortium investigating environment, climate, and health. Environ. Epidemiol. 8, e339.
Gautam, S., 2020. COVID-19: air pollution remains low as people stay at home. Air Qual. Atmos. Health 13, 853–857. https://doi.org/10.1007/s11869-020-00842-6.
Gautam, S., Hens, L., 2020. COVID-19: impact by and on the environment, health and economy. Environ. Dev. Sustain. 22, 4953–4954. https://doi.org/10.1007/s10668-020-00818-7.
Ge, Y., Zhang, W.B., Wu, X., Ruktanonchai, C.W., Liu, H., Wang, J., Song, Y., Liu, M., Yan, W., Yang, J., Cleary, E., Qader, S.H., Atuhaire, F., Ruktanonchai, N.W., Tatem, A.J., Lai, S., 2022. Untangling the changing impact of non-pharmaceutical interventions and vaccination on European COVID-19 trajectories. Nat. Commun. 13, 3106. https://doi.org/10.1038/s41467-022-30897-1.
Gupta, A., Bherwani, H., Gautam, S., Anjum, S., Musugu, K., Kumar, N., Anshul, A., Kumar, R., 2021. Air pollution aggravating COVID-19 lethality? Exploration in asian cities using statistical models. Environ. Dev. Sustain. 23, 6408–6417. https://doi.org/10.1007/s10668-020-00878-9.
Heymann, D.L., Shindo, N., 2020. COVID-19: what is next for public health? Lancet 395, 542–545. https://doi.org/10.1016/S0140-6736(20)30374-3.
Imai, C., Armstrong, B., Chalabi, Z., Mangtani, P., Hashizume, M., 2015. Time series regression model for infectious disease and weather. Environ. Res. 142, 319–327. https://doi.org/10.1016/j.envres.2015.06.040.
Kim, H., Samet, J.M., Bell, M.L., 2022. Association between short-term exposure to air pollution and COVID-19 mortality: a population-based case-crossover study using individual-level mortality registry confirmed by medical examiners. Environ. Health Perspect. 130, 117006. https://doi.org/10.1289/EHP10836.
Kudo, E., Song, E., Yockey, L.J., Rakib, T., Wong, P.W., Homer, R.J., Iwasaki, A., 2019. Low ambient humidity impairs barrier function and innate resistance against influenza infection. Proc. Natl. Acad. Sci. U S A. 166, 10905–10910. https://doi.org/10.1073/pnas.1902840116.
Lavigne, E., Ryti, N., Gasparrini, A., Sera, F., Weichenthal, S., Chen, H., To, T., Evans, G. J., Sun, L., Dheri, A., Lemogo, L., Kotchi, S.O., Stieb, D., 2023. Short-term exposure to ambient air pollution and individual emergency department visits for COVID-19: a case-crossover study in Canada. Thorax 78, 459–466. https://doi.org/10.1136/thoraxjnl-2021-217602.
Li, W., Wang, J., Huang, W., Yan, Y., Liu, Y., Zhao, Q., Chen, M., Yang, L., Guo, Y., Ma, W., 2024. The association between humidex and tuberculosis: a two-stage modelling nationwide study in China. BMC Public Health 24, 1289. https://doi.org/10.1186/s12889-024-18772-8.
Li, Z., Mao, X., Liu, Q., Song, H., Ji, Y., Xu, D., Qiu, B., Tian, D., Wang, J., 2019. Long-term effect of exposure to ambient air pollution on the risk of active tuberculosis. Int. J. Infect. Dis. 87, 177–184. https://doi.org/10.1016/j.ijid.2019.07.027.
Lin, M.W., Lin, C.H., Chang, J.R., Chiang, H.H., Wu, T.H., Lin, C.S., 2025. The influence of PM2.5 exposure on SARS-CoV-2 infection via modulating the expression of angiotensin converting enzyme II. J. Hazard. Mater. 485, 136887. https://doi.org/10.1016/j.jhazmat.2024.136887.
Liu, C., Chen, R., Sera, F., Vicedo-Cabrera, A.M., Guo, Y., Tong, S., Coelho, M.S.Z.S., Saldiva, P.H.N., Lavigne, E., Matus, P., Valdes Ortega, N., Osorio Garcia, S., Pascal, M., Stafoggia, M., Scortichini, M., Hashizume, M., Honda, Y., Hurtado-Díaz, M., Cruz, J., Nunes, B., Teixeira, J.P., Kim, H., Tobias, A., Íñiguez, C., Forsberg, B., Åström, C., Ragettli, M.S., Guo, Y.-L., Chen, B.-Y., Bell, M.L., Wright, C. Y., Scovronick, N., Garland, R.M., Milojevic, A., Kyselý, J., Urban, A., Orru, H., Indermitte, E., Jaakkola, J.J.K., Ryti, N.R.I., Katsouyanni, K., Analitis, A., Zanobetti, A., Schwartz, J., Chen, J., Wu, T., Cohen, A., Gasparrini, A., Kan, H., 2019. Ambient particulate air pollution and daily mortality in 652 cities. N. Engl. J. Med. 381, 705–715. https://doi.org/10.1056/nejmoa1817364.
Ma, Y., Nobile, F., Marb, A., Dubrow, R., Kinney, P.L., Peters, A., Stafoggia, M., Breitner, S., Chen, K., 2024. Air pollution changes due to COVID-19 lockdowns and attributable mortality changes in four countries. Environ. Int. 187, 108668. https://doi.org/10.1016/j.envint.2024.108668.
Ma, Y., Pei, S., Shaman, J., Dubrow, R., Chen, K., 2021. Role of meteorological factors in the transmission of SARS-CoV-2 in the United States. Nat. Commun. 12, 3602. https://doi.org/10.1038/s41467-021-23866-7.
Ma, Z., Hu, X., Sayer, A.M., Levy, R., Zhang, Q., Xue, Y., Tong, S., Bi, J., Huang, L., Liu, Y., 2016. Satellite-based spatiotemporal trends in PM2.5 concentrations: China, 2004-2013. Environ. Health Perspect. 124, 184–192. https://doi.org/10.1289/ehp.1409481.
Madaniyazi, L., Xerxes, S., 2021. Outdoor air pollution and the onset and exacerbation of asthma. Chronic Dis. Transl. Med. 7, 100–106. https://doi.org/10.1016/j.cdtm.2021.04.003.
Manchanda, C., Kumar, M., Singh, V., Faisal, M., Hazarika, N., Shukla, A., Lalchandani, V., Goel, V., Thamban, N., Ganguly, D., Tripathi, S.N., 2021. Variation in chemical composition and sources of PM2.5 during the COVID-19 lockdown in Delhi. Environ. Int. 153, 106541. https://doi.org/10.1016/j.envint.2021.106541.
Martelletti, L., Martelletti, P., 2020. Air pollution and the novel Covid-19 disease: a putative disease risk factor. SN Compr. Clin. Med. 2, 383–387. https://doi.org/10.1007/s42399-020-00274-4.
Masselot, P., Kan, H., Kharol, S.K., Bell, M.L., Sera, F., Lavigne, E., Breitner, S., Das Neves Pereira Da Silva, S., Burnett, R.T., Gasparrini, A., Brook, J.R., Guo, Y., Honda, Y., Huber, V., Jaakkola, J.J.K., Urban, A., Vicedo-Cabrera, A.M., Orru, H., Maasikmets, M., Pascal, M., Schneider, A., Katsouyanni, K., Samoli, E., Diaz, M.H., Arellano, E.E.F., Rao, S., Madureira, J., Holobaca, I.H., Tobias, A., Íñiguez, C., Forsberg, B., Ragettli, M.S., Zanobetti, A., Schwartz, J., 2024. Air pollution mixture complexity and its effect on PM2.5-related mortality: a multicountry time-series study in 264 cities. Environ. Epidemiol. 8, e342.
McAloon, C., Collins, Á., Hunt, K., Barber, A., Byrne, A.W., Butler, F., Casey, M., Griffin, J., Lane, E., McEvoy, D., Wall, P., Green, M., O'Grady, L., More, S.J., 2020. Incubation period of COVID-19: a rapid systematic review and meta-analysis of

observational research. BMJ Open 10, e039652. https://doi.org/10.1136/bmjopen-2020-039652.
McGregor, G.R., 2012a. Special issue: Universal thermal Comfort Index (UTCI). Int. J. Biometeorol. 56, 419. https://doi.org/10.1007/s00484-012-0546-6.
McGregor, G.R., 2012b. Human biometeorology. Prog. Phys. Geogr. 36, 93–109. https://doi.org/10.1177/0309133311417942.
Min, J., Lee, W., Oh, J., Kang, C., Ha, E., 2025. Comparing the role of relative and absolute humidity in heat-related mortality: a case time-series study in South Korea. Environ. Health Perspect. 133. https://doi.org/10.1289/EHP15827.
Monoson, A., Schott, E., Ard, K., Kilburg-Basnyat, B., Tighe, R.M., Pannu, S., Gowdy, K. M., 2023. Air pollution and respiratory infections: the past, present, and future. Toxicol. Sci. 192, 3–14. https://doi.org/10.1093/toxsci/kfad003.
Moriyama, M., Ichinohe, T., 2019. High ambient temperature dampens adaptive immune responses to influenza a virus infection. Proc. Natl. Acad. Sci. U. S. A. 116, 3118–3125. https://doi.org/10.1073/pnas.1815029116.
Nottmeyer, L., Armstrong, B., Lowe, R., Abbott, S., Meakin, S., O'Reilly, K.M., von Borries, R., Schneider, R., Royé, D., Hashizume, M., Pascal, M., Tobias, A., Vicedo-Cabrera, A.M., Lavigne, E., Correa, P.M., Ortega, N.V., Kynčl, J., Urban, A., Orru, H., Ryti, N., Jaakkola, J., Dallavalle, M., Schneider, A., Honda, Y., Ng, C.F.S., Alahmad, B., Carrasco-Escobar, G., Holobâc, I.H., Kim, H., Lee, W., Íñiguez, C., Bell, M.L., Zanobetti, A., Schwartz, J., Scovronick, N., Coélho, M.de.S.Z.S., Saldiva, P.H.N., Diaz, M.H., Gasparrini, A., Sera, F., 2023. The association of COVID-19 incidence with temperature, humidity, and UV radiation – a global multi-city analysis. Sci. Total Environ. 854, 158636. https://doi.org/10.1016/j.scitotenv.2022.158636.
Nottmeyer, L.N., Sera, F., 2021. Influence of temperature, and of relative and absolute humidity on COVID-19 incidence in England - a multi-city time-series study. Environ. Res. 196, 110977. https://doi.org/10.1016/j.envres.2021.110977.
O'Brien, E., Masselot, P., Sera, F., Roye, D., Breitner, S., Ng, C.F.S., Coelho, M.de.S.Z.S., Madureira, J., Tobias, A., Vicedo-Cabrera, A.M., Bell, M.L., Lavigne, E., Kan, H., Gasparrini, A., Carrasco, G., Chen, B.Y., Entezari, A., Guo, Y., Guo, Y.L., Hashizume, M., Holobaca, I.H., Íñiguez, C., Jaakkola, J.J.K., Kim, H., Lee, W., Li, S., Maasikmets, M., Mayvaneh, F., Nunes, B., Orru, H., Osorio, S., Ragettli, M.S., Ryti, N., Saldiva, P.H.N., Schneider, A., Schwartz, J., Tong, S., Zanobetti, A., 2023. Short-term association between sulfur dioxide and mortality: a multicountry analysis in 399 cities. Environ. Health Perspect. 131, 037002. https://doi.org/10.1289/EHP11112.
Oshitani, H., 2022. COVID lessons from Japan: the right messaging empowers citizens. Nature 605, 589. https://doi.org/10.1038/d41586-022-01385-9.
Peel, M.C., Finlayson, B.L., McMahon, T.A., 2007. Updated world map of the Köppen-Geiger climate classification. Hydrol. Earth Syst. Sci. 11, 1633–1644. https://doi.org/10.5194/hess-11-1633-2007.
Polozov, I.V., Bezrukov, L., Gawrisch, K., Zimmerberg, J., 2008. Progressive ordering with decreasing temperature of the phospholipids of influenza virus. Nat. Chem. Biol. 4, 248–255. https://doi.org/10.1038/nchembio.77.
Rai, M., Stafoggia, M., de'Donato, F., Scortichini, M., Zafeiratou, S., Vazquez Fernandez, L., Zhang, S., Katsouyanni, K., Samoli, E., Rao, S., Lavigne, E., Guo, Y., Kan, H., Osorio, S., Kyselý, J., Urban, A., Orru, H., Maasikmets, M., Jaakkola, J.J.K., Ryti, N., Pascal, M., Hashizume, M., Fook Sheng Ng, C., Alahmad, B., Hurtado Diaz, M., De la Cruz Valencia, C., Nunes, B., Madureira, J., Scovronick, N., Garland, R.M., Kim, H., Lee, W., Tobias, A., Íñiguez, C., Forsberg, B., Åström, C., Maria Vicedo-Cabrera, A., Ragettli, M.S., Leon Guo, Y.L., Pan, S.C., Li, S., Gasparrini, A., Sera, F., Masselot, P., Schwartz, J., Zanobetti, A., Bell, M.L., Schneider, A., Breitner, S., 2023. Heat-related cardiorespiratory mortality: effect modification by air pollution across 482 cities from 24 countries. Environ. Int. 174, 107825. https://doi.org/10.1016/j.envint.2023.107825.
Rittweger, J., Gilardi, L., Baltruweit, M., Dally, S., Erbertseder, T., Mittag, U., Naeem, M., Schmid, M., Schmitz, M.T., Wüst, S., Dech, S., Jordan, J., Antoni, T., Bittner, M., 2022. Temperature and particulate matter as environmental factors associated with seasonality of influenza incidence – an approach using Earth observation-based modeling in a health insurance cohort study from Baden-Württemberg (Germany). Environ. Health 21, 131. https://doi.org/10.1186/s12940-022-00927-y.
Rosti, M.E., Olivieri, S., Cavaiola, M., Seminara, A., Mazzino, A., 2020. Fluid dynamics of COVID-19 airborne infection suggests urgent data for a scientific design of social distancing. Sci. Rep. 10, 22426. https://doi.org/10.1038/s41598-020-80078-7.
Rubin, D., Huang, J., Fisher, B.T., Gasparrini, A., Tam, V., Song, L., Wang, X., Kaufman, J., Fitzpatrick, K., Jain, A., Griffis, H., Crammer, K., Morris, J., Tasian, G., 2020. Association of social distancing, population density, and temperature with the instantaneous reproduction number of SARS-CoV-2 in counties across the United States. JAMA Netw. Open 3, e2016099–e. https://doi.org/10.1001/jamanetworkopen.2020.16099.
Sarkodie, S.A., Owusu, P.A., 2020. Impact of meteorological factors on COVID-19 pandemic: evidence from top 20 countries with confirmed cases. Environ. Res. 191, 110101. https://doi.org/10.1016/j.envres.2020.110101.
Scialo, F., Daniele, A., Amato, F., Pastore, L., Matera, M.G., Cazzola, M., Castaldo, G., Bianco, A., 2020. ACE2: the major cell entry receptor for SARS-CoV-2. Lung 198, 867–877. https://doi.org/10.1007/s00408-020-00408-4.
Sera, F., Armstrong, B., Abbott, S., Meakin, S., O'Reilly, K., von Borries, R., Schneider, R., Royé, D., Hashizume, M., Pascal, M., Tobias, A., Vicedo-Cabrera, A.M., Hu, W., Tong, S., Lavigne, E., Correa, P.M., Meng, X., Kan, H., Kynčl, J., Urban, A., Orru, H., Ryti, N.R.I., Jaakkola, J.J.K., Cauchemez, S., Dallavalle, M., Schneider, A., Zeka, A., Honda, Y., Ng, C.F.S., Alahmad, B., Rao, S., Di Ruscio, F., Carrasco-Escobar, G., Seposo, X., Holobâcă, I.H., Kim, H., Lee, W., Íñiguez, C., Ragettli, M.S., Aleman, A., Colistro, V., Bell, M.L., Zanobetti, A., Schwartz, J., Dang, T.N., Scovronick, N., de Sousa Zanotti Stagliorio Coélho, M., Diaz, M.H., Zhang, Y., Russell, T.W., Koltai, M., Kucharski, A.J., Barnard, R.C., Quaife, M., Jarvis, C.I., Lei, J., Munday, J.D., Chan, Y. W.D., Quilty, B.J., Eggo, R.M., Flasche, S., Foss, A.M., Clifford, S., Tully, D.C., Edmunds, W.J., Klepac, P., Brady, O., Krauer, F., Procter, S.R., Jombart, T., Rosello, A., Showering, A., Funk, S., Hellewell, J., Sun, F.Y., Endo, A., Williams, J., Gimma, A., Waterlow, N.R., Prem, K., Bosse, N.I., Gibbs, H.P., Atkins, K.E., Pearson, C.A.B., Jafari, Y., Villabona-Arenas, C.J., Jit, M., Nightingale, E.S., Davies, N.G., van Zandvoort, K., Liu, Y., Sandmann, F.G., Waites, W., Abbas, K., Medley, G., Knight, G.M., Gasparrini, A., Lowe, R., 2021. A cross-sectional analysis of meteorological factors and SARS-CoV-2 transmission in 409 cities across 26 countries. Nat. Commun. 12, 5968. https://doi.org/10.1038/s41467-021-25914-8.
Sera, F., Armstrong, B., Blangiardo, M., Gasparrini, A., 2019. An extended mixed-effects framework for meta-analysis. Stat. Med. 38, 5429–5444. https://doi.org/10.1002/sim.8362.
Sera, F., Gasparrini, A., 2022. Extended two-stage designs for environmental research. Environ. Health 21, 41. https://doi.org/10.1186/s12940-022-00853-z.
Spinner, C.D., Bell, S., Einsele, H., Tremblay, C., Goldman, M., Chagla, Z., Finckh, A., Edwards, C.J., Aurer, I., Launay, O., Casañas i Comabella, C., James, S., Dube, S., Borkowska, K., Jah, F., Kandeil, W., Yokota, R.T.C., Artaud, C., Gottenberg, J.E., Gesualdo, L., Bertrand, D., Arnetorp, S., Magiorkinis, G., 2025. Is COVID-19 still a threat? an expert opinion review on the continued healthcare burden in immunocompromised individuals. Adv. Ther. 42, 666–719. https://doi.org/10.1007/s12325-024-03043-0.
Stafoggia, M., Ranzi, A., Ancona, C., Bauleo, L., Bella, A., Cattani, G., Nobile, F., Pezzotti, P., Iavarone, I., 2023. Long-term exposure to ambient air pollution and mortality among four million COVID-19 cases in Italy: the EpiCovAir study. Environ. Health Perspect. 131, 057004. https://doi.org/10.1289/EHP11882.
Thi Khanh, H.N., De Troeyer, K., Smith, P., Demoury, C., Casas, L., 2024. The impact of ambient temperature and air pollution on SARS-CoV2 infection and Post COVID-19 condition in Belgium (2021–2022). Environ. Res. 246, 118066. https://doi.org/10.1016/j.envres.2023.118066.
Urban, A., Di Napoli, C., Cloke, H.L., Kyselý, J., Pappenberger, F., Sera, F., Schneider, R., Vicedo-Cabrera, A.M., Acquaotta, F., Ragettli, M.S., Íñiguez, C., Tobias, A., Indermitte, E., Orru, H., Jaakkola, J.J.K., Ryti, N.R.I., Pascal, M., Huber, V., Schneider, A., de' Donato, F., Michelozzi, P., Gasparrini, A., 2021. Evaluation of the ERA5 reanalysis-based Universal thermal climate Index on mortality data in Europe. Environ. Res. 198, 111227. https://doi.org/10.1016/j.envres.2021.111227.
Venter, Z.S., Aunan, K., Chowdhury, S., Lelieveld, J., 2020. COVID-19 lockdowns cause global air pollution declines. Proc. Natl. Acad. Sci. U S A. 117, 18984–18990. https://doi.org/10.1073/pnas.2006853117.
Wang, Y., Lyu, Y., Tong, S., Ding, C., Wei, L., Zhai, M., Xu, K., Hao, R., Wang, X., Li, N., Luo, Y., Li, Y., Wang, J., 2023. Association between meteorological factors and COVID-19 transmission in low- and middle-income countries: a time-stratified case-crossover study. Environ. Res. 231, 116088. https://doi.org/10.1016/j.envres.2023.116088.
Wei, Y., Dong, Z., Fan, W., Xu, K., Tang, S., Wang, Y., Wu, F., 2022. A narrative review on the role of temperature and humidity in COVID-19: Transmission, persistence, and epidemiological evidence. Eco-Environ. Health 1, 73–85. https://doi.org/10.1016/j.eehl.2022.04.006.
World Health Organization, n.d. Coronavirus disease (COVID-19) epidemiological updates and monthly operational updates. Retrieved from https://www.who.int/emergencies/diseases/novel-coronavirus-2019/situation-reports. Accessed June 20, 2025.
Wu, X., Nethery, R.C., Sabath, M.B., Braun, D., Dominici, F., 2020a. Air pollution and COVID-19 mortality in the United States: Strengths and limitations of an ecological regression analysis. Sci. Adv. 6, eabd4049. https://doi.org/10.1126/SCIADV.ABD4049.
Wu, Y., Jing, W., Liu, J., Ma, Q., Yuan, J., Wang, Y., Du, M., Liu, M., 2020b. Effects of temperature and humidity on the daily new cases and new deaths of COVID-19 in 166 countries. Sci. Total Environ. 729, 139051. https://doi.org/10.1016/j.scitotenv.2020.139051.
Wu, Y., Kang, L., Guo, Z., Liu, J., Liu, M., Liang, W., 2022. Incubation period of COVID-19 caused by unique SARS-CoV-2 strains: a systematic review and meta-analysis. JAMA Netw. Open 5, e2228008–e. https://doi.org/10.1001/jamanetworkopen.2022.28008.
Xu, K., Li, Q., Cao, Y. qin, Ma, L., Zhang, X. song, Yu, J. ze, Liu, M. xin, Zhu, A. ning, Tian, T., Ruan, Y., 2025. The impact of high humidex on the risk of hospital admissions for urinary system diseases in Lanzhou, China: A time-series analysis. iScience. 28. Doi: 10.1016/j.isci.2025.111968.
Xu, R., Rahmandad, H., Gupta, M., DiGennaro, C., Ghaffarzadegan, N., Amini, H., Jalali, M.S., 2021. Weather, air pollution, and SARS-CoV-2 transmission: a global analysis. Lancet Planet. Health. 5, e671–e680. https://doi.org/10.1016/S2542-5196(21)00202-3.
Yan, X., Du, Y., Li, K., Zhao, X., Wang, H., Liu, L., Wang, Q., Liu, J., Wei, S., 2025. Effects of long-term air pollution exposure on disease outcomes and hybrid immune responses in SARS-CoV-2 breakthrough infections: a study of the Yichang COVID-19 Antibody Longitudinal Survey (YC-CALS) in China. Environ. Health Perspect. 133, 57022. https://doi.org/10.1289/EHP15660.
Yu, K., Zhang, Q., Wei, Y., Chen, R., Kan, H., 2024a. Global association between air pollution and COVID-19 mortality: a systematic review and meta-analysis. Sci. Total Environ. 906, 167542. https://doi.org/10.1016/j.scitotenv.2023.167542.
Yu, W., Huang, W., Gasparrini, A., Sera, F., Schneider, A., Breitner, S., Kyselý, J., Schwartz, J., Madureira, J., Gaio, V., Guo, Y.L., Xu, R., Chen, G., Yang, Z., Wen, B., Wu, Y., Zanobetti, A., Kan, H., Song, J., Li, S., Guo, Y., Tong, S., Pascal, M., Das Neves Pereira Da Silva, S., Tobias, A., Íñiguez, C., Pan, S.C., Urban, A., Jaakkola, J.J. K., Ryti, N., Ameling, C., Houthuijs, D., Rao, S., Forsberg, B., Scortichini, M., Stafoggia, M., Masselot, P., 2024b. Ambient fine particulate matter and daily

mortality: a comparative analysis of observed and estimated exposure in 347 cities. Int. J. Epidemiol. 53, dyae066. https://doi.org/10.1093/ije/dyae066.
Yu, W., Li, S., Ye, T., Xu, R., Song, J., Guo, Y., 2022. Deep ensemble machine learning framework for the estimation of $PM_{2.5}$ concentrations. Environ. Health Perspect. 130, 037004. https://doi.org/10.1289/EHP9752.
Yu, W., Xu, R., Ye, T., Abramson, M.J., Morawska, L., Jalaludin, B., Johnston, F.H., Henderson, S.B., Knibbs, L.D., Morgan, G.G., Lavigne, E., Heyworth, J., Hales, S., Marks, G.B., Woodward, A., Bell, M.L., Samet, J.M., Song, J., Li, S., Guo, Y., 2024c. Estimates of global mortality burden associated with short-term exposure to fine particulate matter ($PM_{2.5}$). Lancet Planet. Health. 8, e146–e155. https://doi.org/10.1016/S2542-5196(24)00003-2.
Yu, W., Ye, T., Zhang, Y., Xu, R., Lei, Y., Chen, Z., Yang, Z., Zhang, Y., Song, J., Yue, X., Li, S., Guo, Y., 2023. Global estimates of daily ambient fine particulate matter concentrations and unequal spatiotemporal distribution of population exposure: a machine learning modelling study. Lancet Planet. Health. 7, e209–e218. https://doi.org/10.1016/S2542-5196(23)00008-6.
Yuan, J., Wu, Y., Jing, W., Liu, J., Du, M., Wang, Y., Liu, M., 2021. Non-linear correlation between daily new cases of COVID-19 and meteorological factors in 127 countries. Environ. Res. 193, 110521. https://doi.org/10.1016/j.envres.2020.110521.
Zhan, Z.Y., Fang, H.Y., Xu, X.Y., Hu, Z.J., 2023. Interactions of particulate matter with temperature, heat index and relative humidity on pediatric hand, foot, and mouth disease in a subtropical city. Environ. Pollut. 336, 122385. https://doi.org/10.1016/j.envpol.2023.122385.
Zhang, C., Liao, H., Strobl, E., Li, H., Li, R., Jensen, S.S., Zhang, Y., 2021. The role of weather conditions in COVID-19 transmission: a study of a global panel of 1236 regions. J. Clean. Prod. 292, 125987. https://doi.org/10.1016/j.jclepro.2021.125987.
Zhang, J., Lim, Y.H., So, R., Jørgensen, J.T., Mortensen, L.H., Napolitano, G.M., Cole-Hunter, T., Loft, S., Bhatt, S., Hoek, G., Brunekreef, B., Westendorp, R., Ketzel, M., Brandt, J., Lange, T., Kølsen-Fisher, T., Andersen, Z.J., 2023a. Long-Term exposure to air pollution and risk of SARS-CoV-2 infection and COVID-19 hospitalisation or death: danish nationwide cohort study. Eur. Respir. J. 62, 2300280. https://doi.org/10.1183/13993003.00280-2023.
Zhang, R., Lai, K.Y., Liu, W., Liu, Y., Ma, X., Webster, C., Luo, L., Sarkar, C., 2023b. Associations between short-term exposure to ambient air pollution and influenza: an individual-level case-crossover study in Guangzhou. China. Environ. Health Perspect. 131, 127009. https://doi.org/10.1289/EHP12145.
Zhao, R., Gao, Q., Hao, Q., Wang, S., Zhang, Y., Li, H., Jiang, B., 2021. The exposure-response association between humidex and bacillary dysentery: a two-stage time series analysis of 316 cities in mainland China. Sci. Total Environ. 797, 148840. https://doi.org/10.1016/j.scitotenv.2021.148840.
Zhu, Y., Xie, J., Huang, F., Cao, L., 2020. Association between short-term exposure to air pollution and COVID-19 infection: evidence from China. Sci. Total Environ. 727, 138704. https://doi.org/10.1016/j.scitotenv.2020.138704.

Glossary

SARS-CoV-2: severe acute respiratory syndrome coronavirus 2
COVID-19: coronavirus disease 2019
NPIs: non-pharmaceutical interventions
WBGT: wet-bulb globe temperature
UTCI: universal thermal climate index
HFMD: hand, foot, and mouth disease;
$PM_{2.5}$: fine particulate matter $\leq$ 2.5 μm
PM_{10}: fine particulate matter $\leq$ 10 μm
CO: carbon monoxide
NO_2: nitrogen dioxide
O_3: ozone
MCC: Multi-Country Multi-City
PHSMs: public health and social measures
GSI: Government Stringency Index
OxCGRT: Oxford COVID-19 Government Response Tracker
qAIC: quasi-Akaike information criterion
df: degrees of freedom
RRs: relative risks
CIs: confidence intervals
AN: attributable number
AF: attributable fraction
eCIs: empirical confidence intervals
RRRs: ratio of relative risks
ACE2: angiotensin-converting enzyme 2